Air Force Space Command

SPACE AND MISSILE SYSTEMS CENTER STANDARD

END-OF-LIFE DISPOSAL OF SATELLITES IN LOW-EARTH ORBIT

Report Documentation Page		*Form Approved* *OMB No. 0704-0188*

Public reporting burden for the collection of information is estimated to average 1 hour per response, including the time for reviewing instructions, searching existing data sources, gathering and maintaining the data needed, and completing and reviewing the collection of information. Send comments regarding this burden estimate or any other aspect of this collection of information, including suggestions for reducing this burden, to Washington Headquarters Services, Directorate for Information Operations and Reports, 1215 Jefferson Davis Highway, Suite 1204, Arlington VA 22202-4302. Respondents should be aware that notwithstanding any other provision of law, no person shall be subject to a penalty for failing to comply with a collection of information if it does not display a currently valid OMB control number.

1. REPORT DATE **19 MAR 2010**	2. REPORT TYPE **N/A**	3. DATES COVERED **-**

4. TITLE AND SUBTITLE **SMC-S-022 (2010) End-of-Life Disposal of Satellites in Low-Earth Orbit**		5a. CONTRACT NUMBER
		5b. GRANT NUMBER
		5c. PROGRAM ELEMENT NUMBER
6. AUTHOR(S)		5d. PROJECT NUMBER
		5e. TASK NUMBER
		5f. WORK UNIT NUMBER
7. PERFORMING ORGANIZATION NAME(S) AND ADDRESS(ES) **USAF Space and Missile Systems Center**		8. PERFORMING ORGANIZATION REPORT NUMBER
9. SPONSORING/MONITORING AGENCY NAME(S) AND ADDRESS(ES)		10. SPONSOR/MONITOR'S ACRONYM(S)
		11. SPONSOR/MONITOR'S REPORT NUMBER(S)

12. DISTRIBUTION/AVAILABILITY STATEMENT
Approved for public release, distribution unlimited

13. SUPPLEMENTARY NOTES

14. ABSTRACT

15. SUBJECT TERMS

16. SECURITY CLASSIFICATION OF:			17. LIMITATION OF ABSTRACT **UU**	18. NUMBER OF PAGES **47**	19a. NAME OF RESPONSIBLE PERSON
a. REPORT **unclassified**	b. ABSTRACT **unclassified**	c. THIS PAGE **unclassified**			

Standard Form 298 (Rev. 8-98)
Prescribed by ANSI Std Z39-18

FOREWORD

1.   This standard defines the Government's requirements and expectations for contractor performance in defense system acquisitions and technology developments.

2.   This new-issue SMC standard comprises the text of The Aerospace Corporation report number TOR-2007(8506)-7164, entitled *Requirements for End-Of-Life Disposal of Satellites Operating in Orbits with Perigees below 2000 Kilometers.*

3.   Beneficial comments (recommendations, changes, additions, deletions, etc.) and any pertinent data that may be of use in improving this standard should be forwarded to the following addressee using the Standardization Document Improvement Proposal appearing at the end of this document or by letter:

<div align="center">

Division Chief, SMC/EAE
SPACE AND MISSILE SYSTEMS CENTER
Air Force Space Command
483 N. Aviation Blvd.
El Segundo, CA 90245

</div>

4.   This standard has been approved for use on all Space and Missile Systems Center/Air Force Program Executive Office - Space development, acquisition, and sustainment contracts.

<div align="center">

DAVID E. SWANSON, COL, USAF
SMC Chief Engineer

</div>

Contents

Figures

Tables

1. Scope

According to the U.S. Government Orbital Debris Standard Practices, [1] a spacecraft or upper stage with perigee altitude below 2000 km in its final mission orbit may be disposed of by using an atmospheric reentry option. The guideline for atmospheric reentry is stated as follows:

> *"Leave the structure in an orbit in which, using conservative projections for solar activity, atmospheric drag will limit the lifetime to no longer than 25 years after completion of mission. If drag enhancement devices are to be used to reduce the orbit lifetime, it should be demonstrated that such devices will significantly reduce the area-time product of the system or will not cause spacecraft or large debris to fragment if a collision occurs while the system is decaying from orbit."*

The Inter-Agency Space Debris Coordination Committee (IADC) Space Debris Mitigation Guidelines[2] state:

"Whenever possible space systems that are terminating their operational phases in orbits that pass through the LEO region, or have the potential to interfere with the LEO region, should be de-orbited (direct re-entry is preferred) or where appropriate maneuvered into an orbit with a reduced lifetime. Retrieval is also a disposal option.

A space system should be left in an orbit in which, using an accepted nominal projection for solar activity, atmospheric drag will limit the orbital lifetime after completion of operations. A study on the effect of post-mission orbital lifetime limitation on collision rate and debris population growth has been performed by the IADC. This IADC and some other studies and a number of existing national guidelines have found 25 years to be a reasonable and appropriate lifetime limit. If a space system is to be disposed of by re-entry into the atmosphere, debris that survives to reach the surface of the Earth should not pose an undue risk to people or property. This may be accomplished by limiting the amount of surviving debris or confining the debris to uninhabited regions, such as broad ocean areas. Also, ground environmental pollution, caused by radioactive substances, toxic substances or any other environmental pollutants resulting from on-board articles, should be prevented or minimized in order to be accepted as permissible.

In the case of a controlled re-entry of a space system, the operator of the system should inform the relevant air traffic and maritime traffic authorities of the re-entry time and trajectory and the associated ground area."

This report specifies requirements for (1) planning for disposal of satellites operating in low Earth orbits with perigee altitude below 2000 km, (2) selecting the final disposal orbits whose perigee altitude is low enough to ensure a natural decay due to atmospheric drag within 25 years, (3) executing the disposal maneuver successfully, and (4) depleting all energy sources onboard the vehicle prior to end-of-life to minimize the possibility of a debris-producing event. Techniques for planning and determining the final disposal orbit are provided, considering current internationally accepted guidelines and operational best practices.

2. Application

These requirements shall be applied to the end-of-life disposal of satellites operating in LEO (Low Earth Orbit) or HEO (Highly Elliptical Orbit) with low perigee altitudes ($H_p < 2000$ km). The requirements are applicable to all DOD/NASA/NOAA/civil space programs with perigee altitude

lower than 2000 km, such as DMSP, NPOESS, Iridium, Molniya, and GTO (Geosynchronous Transfer Orbit) rocket bodies.

3. Terms and Definitions

- **End of Life (EOL):** The point in time at which a satellite is permanently turned off (nominally after the space system has been placed in a disposal orbit) or when control of the satellite from the ground is no longer possible.

- **End of Mission:** End of mission refers to the completion of the scheduled mission of the space system, or when the mission is halted either because of a failure in space or a voluntary decision.

- **LEO Region:** The LEO region is a spherical region that extends from the Earth's surface up to an altitude of 2,000 km. .

- **Drag Enhancement Device:** A drag enhancement device on a spacecraft effectively increases the cross-sectional area of the spacecraft and thereby increases the atmospheric drag effect to shorten the decay time. One such effective device is the balloon.

- **Direct Reentry:** Without using the atmospheric drag decay, the spacecraft is inserted into an orbit with perigee low enough to ensure a ground impact after a half revolution of the orbit.

4. Symbols and Acronyms

a	Orbit semimajor axis
A	Satellite cross-sectional area with respect to the relative wind
A_p	Earth daily geomagnetic index
β	Ballistic coefficient of satellite $= C_D * A / m$
C_D	Satellite drag coefficient
e	Orbit eccentricity
EOL	End of life
$F10.7$	Solar radio flux observed daily at 2800 MHz (10.7 cm) in solar flux units $(10^{-22} \text{ W m}^{-2} \text{ Hz}^{-1})$
$F10.7 Bar$	Solar radio flux at 2800 MHz (10.7 cm), averaged over three solar rotations
GEO	Geosynchronous Earth orbit
H_a	Apogee altitude $= a (1 + e) - R_e$
H_p	Perigee altitude $= a (1 – e) - R_e$
$IADC$	Inter-Agency Space Debris Coordination Committee
ISO	International Standard Organization
LEO	Low Earth orbit
m	Mass of satellite
$RAAN$	Orbit Right Ascension of the Ascending Node; the angle between the vernal equinox and the orbit ascending node, measured counter-clockwise in the equatorial plane, looking in the –Z direction.
R_e	Equatorial radius of the Earth $= 6378.137$ km

5. Primary Requirements

5.1 Disposal Maneuver Planning

An "End of Mission Disposal Plan" (EOMDP) shall be developed, maintained, and updated in all phases of mission and spacecraft design and operations. An accurate estimate of fuel shall be required to ensure orbit decay within 25 years. This document shall include:

- Details of the nominal mission orbit
- Details of the targeted disposal orbit
- Estimates of the fuel required for the disposal action
- Identity of system and capabilities required for successful completion of the disposal action
- Criteria that dictate initiation of the disposal action when met
- Identities of energy sources that must be depleted prior to end-of-life
- A timeline for initiation and execution of the disposal action
- A timeline for depletion of remaining energy sources
- A list of those individuals and/or entities to be notified of the end-of-mission and disposal and a timeline for notification

5.2 Reliability for Disposal

The space system shall be designed such that the probability of successful end-of-mission disposal, including depletion of energy sources, equals or exceeds 0.9 at end of design mission life. The disposal success probability shall be evaluated as conditional probability (weighted on the mission success). Appendix E provides a discussion of the conditional probability. Details of the design that provide the basis for the probability estimate shall be included in the EOMDP.

5.3 Criteria for Executing Disposal Action

Specific criteria for initiation of the disposal action shall be developed, included in the EOMDP, and monitored throughout the mission life. Projections of mission life based on these criteria shall be a regular part of mission status reviews during the mission. The status of these criteria shall be presented at periodic (at least yearly) mission reviews.

5.4 Energy Depletion Planning

Independent of the success or failure of other aspects of the disposal action, a plan shall be developed to deplete all energy sources, and safe the vehicle in accordance with ISO passivation standards before the final demise of the spacecraft. (Passivation or safing is the elimination of all stored energy on a spacecraft or orbital stages to reduce the chance of break-up. Typical passivation measures include venting or burning excess propellant, discharging batteries, and relieving pressure vessels.) The objective shall be to ensure that actions necessary to safe the vehicle are taken before critical systems are lost. The plan shall include criteria that define when the safing actions are to be taken, the rationale for each criterion, and a schedule for safing actions. The plan shall be included in the EOMDP.

6. Disposal Planning Requirements

Planning activities for end-of-mission disposal shall start in mission design. Planning for the actual disposal action shall begin at least six months prior to the date of re-orbit maneuvers. The following steps shall be followed in all mission phases and shall be documented in the EOMDP.

6.1 Estimate Ballistic Coefficient (C_dA/m) Considering Tumbling

The first step in planning for the disposal of a LEO or HEO spacecraft is to estimate the ballistic coefficient (C_dA/m) considering spacecraft tumbling. It is generally believed that the average value between the maximum and minimum cross-section area should be used to compute the ballistic coefficient of a tumbling spacecraft. The proper value of the dimensionless drag coefficient, C_d, is 2 for a typical spacecraft. A discussion on the drag coefficient is given in Appendix A.

6.2 Determine Orbit Lifetime of Nominal Mission Orbit

The second step is to predict the orbit lifetime of the nominal mission orbit beginning at the end-of-life. No further planning is required if the predicted orbit lifetime based on one of the following recommended methods is within 25 years. See Section 6.3 if the predicted lifetime is longer than 25 years.

To predict orbit lifetime:

- Perform long-term orbit propagations using either semi-analytical or numerical integration tools. Choose the up-to-date atmospheric density model, such as JB2006 or MSISE00. The recommended long-term propagation tools and the solar flux data are discussed in detail in Section 7 and 8.
- Determine orbit lifetime from the empirical equations provided in Appendix B. These empirical equations are not applicable to the three special orbit types: sun-synchronous orbits, Molniya orbits and Magic orbits. These orbits are discussed in Appendix D. The long-term lifetime prediction should be performed using semi-analytical or numerical integration tools as in a) above.

6.3 Determine the Strategy for Ensuring 25-Year Lifetime

There are two basic strategies to ensure a 25-year lifetime if the nominal mission orbit lifetime is longer than 25 years. The first strategy is to perform maneuvers to lower the orbit altitude to achieve the 25-year lifetime. The second strategy is to use drag enhancement devices, such as balloons or parachutes.

6.3.1 Lower Orbit Altitude

The recommended strategy to lower the orbit altitude is to perform a single-burn at apogee to lower the perigee altitude to the predetermined value that ensures a 25-year lifetime. It has been proven through numerical simulations that a single-burn maneuver requires less propellant than a two-burn Hohmann type transfer to ensure a lifetime less than 25 years.

The procedure to determine the amount of ΔV required is through either numerical orbit propagation or table lookup, as discussed in section 6.2 above. The single burn should be executed near a predetermined time such that the new argument of perigee is at or close to 270 deg. This optimum

eccentricity vector[3] can shorten the 25-year lifetime by 1 to 20 percent, depending on initial eccentricity and perigee altitude. Consequently, the amount of required ΔV for ensuring decay within 25 years may be significantly reduced.

6.3.2 Use Drag Enhancement Devices

This strategy requires the use of drag enhancement devices, such as balloons or parachutes. The average ballistic coefficient of the spacecraft with drag enhancement device deployed must be estimated. The new ballistic coefficient (C_DA/m) is determined by iteration using either one of the two methods described in Section 6.2. This strategy may also require an apogee burn to lower the perigee, depending on the effectiveness of the drag device. In this strategy, the deployment of the drag device and the apogee burn, if needed, should also be timed as discussed in a) for achieving the initial optimum eccentricity vector. An assessment of the drag enhancement device is recommended to demonstrate that either the device will significantly reduce the collision risk of the system by the reduction of the orbit lifetime or that the device will not cause spacecraft or large debris to fragment if a collision occurs while the system is decaying from orbit.

6.4 Develop Basic Maneuver Requirements for Achieving Disposal Orbit

The mission operations shall develop maneuver sequences to achieve the predetermined disposal orbit and to assure that drag enhancement devices are properly deployed if this strategy is used. The predetermined disposal orbit shall satisfy the following conditions:

- The perigee altitude must be low enough to ensure that the spacecraft shall decay through atmospheric drag within 25 years.
- The argument of perigee shall be either close to 270 deg or the estimated value of the optimum eccentricity vector.

In all cases, the space system shall be passivated prior to end of life.

7. Orbit Lifetime Assessment

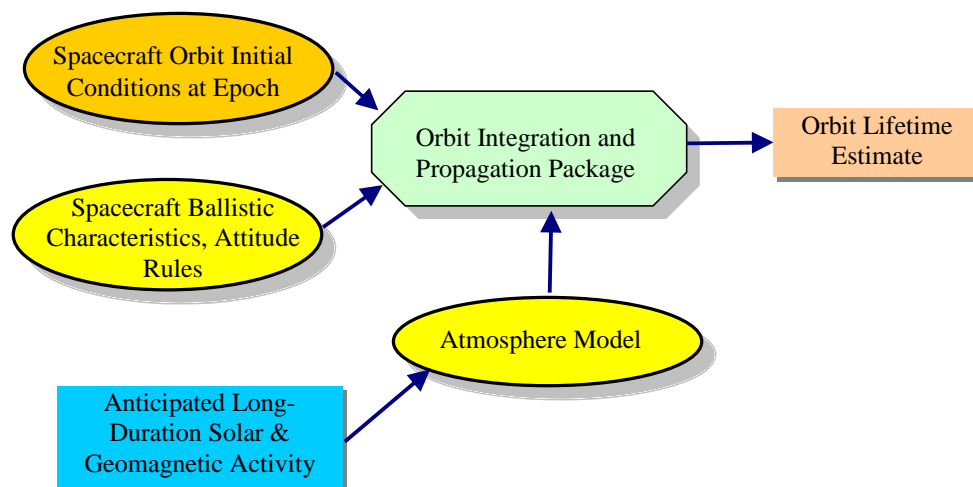The orbit lifetime estimation process is represented generically in Figure 1.

Figure 1. Orbit lifetime assessment process.

7.1 Orbit Lifetime Assessment Methods and Applicability

There are three basic analysis methods used to estimate orbit lifetime. Method 1 is simply a table lookup, graphical analysis, or evaluation of equations fit to pre-computed orbit lifetime estimation data obtained via the extensive and repetitive application of Methods 2 and/or 3. Method 2 utilizes a definition of mean orbital elements[4,5] semi-analytic orbit theory and average satellite ballistic coefficient to permit the very rapid integration of the equations of motion, while still retaining reasonable accuracy. Method 3, clearly the highest fidelity model, utilizes a numerical integrator with a detailed gravity model, third-body effects, solar radiation pressure, and a detailed satellite ballistic coefficient model.

7.1.1 Method 1: Numerical Table Look-up, Analysis and Fit Equation Evaluations

In this first method, one uses tables, graphs and equations representing data that was generated by exhaustively using Methods 2 and 3 (see below). The tables, graphs and equations provided in this report can help the analyst assess orbit lifetime for their particular case of interest; all such Method 1 data in this report were generated using Method 2 approaches.

7.1.2 Method 2: Rapid Semianalytical Orbit Propagation

Method 2 analysis tools utilize semianalytic propagation of mean orbit elements[4,5] influenced by gravity zonals J_2 and J_3 and selected atmosphere models. The primary advantage of this approach over direct three-dimensional numerical integration of the equations of motion (Method 3) is that long-duration orbit lifetime cases can be quickly analyzed (e.g., 5 seconds CPU time for a 30-year orbit lifetime case). While incorporation of an attitude-dependent ballistic coefficient is doable for this method, an average ballistic coefficient is typically used.

The Method 2 results provided in this report were generated using the LIFETIME program,[6,7,8] developed and maintained by The Aerospace Corporation, and the QPROP program, developed and maintained by 1Earth Research, LLC. Both tools are PC-based, use Method 2-type orbit lifetime estimators, using semi-analytic propagation of mean orbit elements coupled with gravity zonals J_2 and J_3 and selected atmosphere models (including MSISE2000, Jacchia-Bowman 2006, Jacchia 1971, etc.). The LIFETIME analysis tool has been used to analyze orbit lifetime and satellite reentry by various Government and industrial organizations. Its accuracy has been validated by high-precision numerical integration results (Method 3 type) as well as actual satellite decay data.

The LIFETIME and QPROP software tools were exercised in this study to jointly analyze over eight million orbit lifetime cases, spanning a variety of times-into-the-solar-cycle, inclinations, perigee altitudes (H_p), apogee altitudes (H_a), and ballistic coefficients.

7.1.3 Method 3: High-precision numerical integration

Method 3 is the direct numerical integration of all accelerations in Cartesian space, with the ability to incorporate a detailed gravity model (e.g., using a larger spherical harmonics model to address resonance effects), third-body effects, solar radiation pressure, vehicle attitude rules or aero-torque-driven attitude torques, and a detailed satellite ballistic coefficient model based on the angle-of-attack with respect to the relative wind. Atmospheric rotation at the Earth's rotational rate is also easily incorporated in this approach. The only negative aspects to such simulations are (1) they run much slower than Method 2; (2) many of the detailed data inputs required to make Method 3 realize its full accuracy potential are not available; and (3) any gains in orbit lifetime prediction accuracy are

frequently overwhelmed by inherent inaccuracies of atmospheric modeling. However, this is undoubtedly the most accurate method to analyze a few select cases where such detailed model inputs are known.

8.   Atmospheric Density Modeling

The three biggest factors in orbit lifetime estimation are (1) the selection of an appropriate atmosphere model to incorporate into the orbit acceleration formulation; (2) the selection of appropriate inputs to such a model; and (3) ballistic coefficient determination.

8.1   Atmospheric Drag Models

A wide variety of atmosphere models are available to the orbit analyst. The background, technical basis, utility and functionality of these atmosphere models are described in detail in Ref. 9. This report does not presume to dictate which atmosphere model the analyst shall use. However, it is worth noting that in general, the heritage, expertise and especially the observational data that went into creating each atmosphere model play a key role in that model's ability to predict atmospheric density, which is in turn a key factor in estimating orbit lifetime. Many of the early atmosphere models were low fidelity and were created on the basis of only one, or perhaps even just a part of one, solar cycle's worth of data.

The advantage of some of these early models is that they typically run much faster than the latest high-fidelity models (see Figure 2) without losing a great deal of accuracy. However, the use of atmosphere models that were designed to fit a select altitude range (e.g., the "exponential" atmosphere model shown in Figure 2) or models that do not accommodate solar activity variations should be avoided, as they miss too many atmospheric density variations to be sufficiently accurate.

There are some early models (e.g., the Jacchia 1971[10]) that do accommodate solar activity variations yet run very fast; these models, while perhaps not ideal, can work well for long-duration orbit lifetime studies where numerous cases are to be examined. A crude comparison of a sampling of atmosphere models for a single test case is shown in Figures 3 and 4, illustrating the range of temperatures and densities exhibited by the various models.

Use of the more recent atmosphere models (e.g., MSISE2000[11] and Jacchia-Bowman[12]) are encouraged because they have substantially more atmospheric drag data incorporated as the foundation of their underlying assumptions. A recent study by Marcos, et al.[13], indicates that the standard deviations for the JB2006 model are lower at all altitudes. Both the improved solar indices and semiannual formulations contribute, approximately equally, to the successful increase in JB2006 model precision.

Atmosphere Model	CPU sec 0<Alt<5000 km	CPU sec 0<Alt<1000 km
Exponential	0.578	0.547
Atm1962	0.829	0.828
Atm1976	0.89	0.844
Jacchia 1971	7.906	9.468
MSIS 2000	81.547	121.875
JB2006	395.266	319.704

Figure 2. Atmosphere model runtime (1M evals).
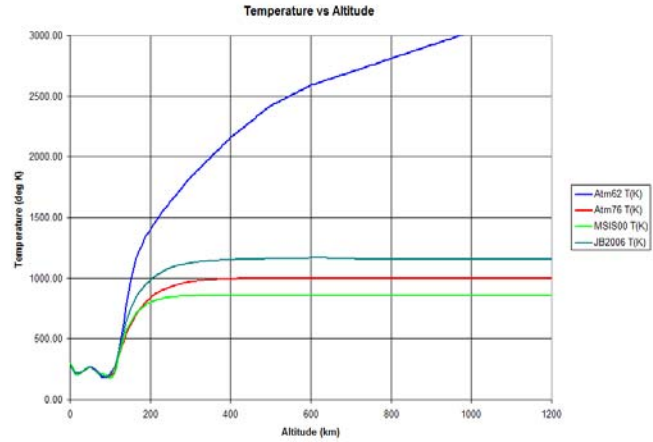
Figure 3. Temperature comparison by atmosphere model.
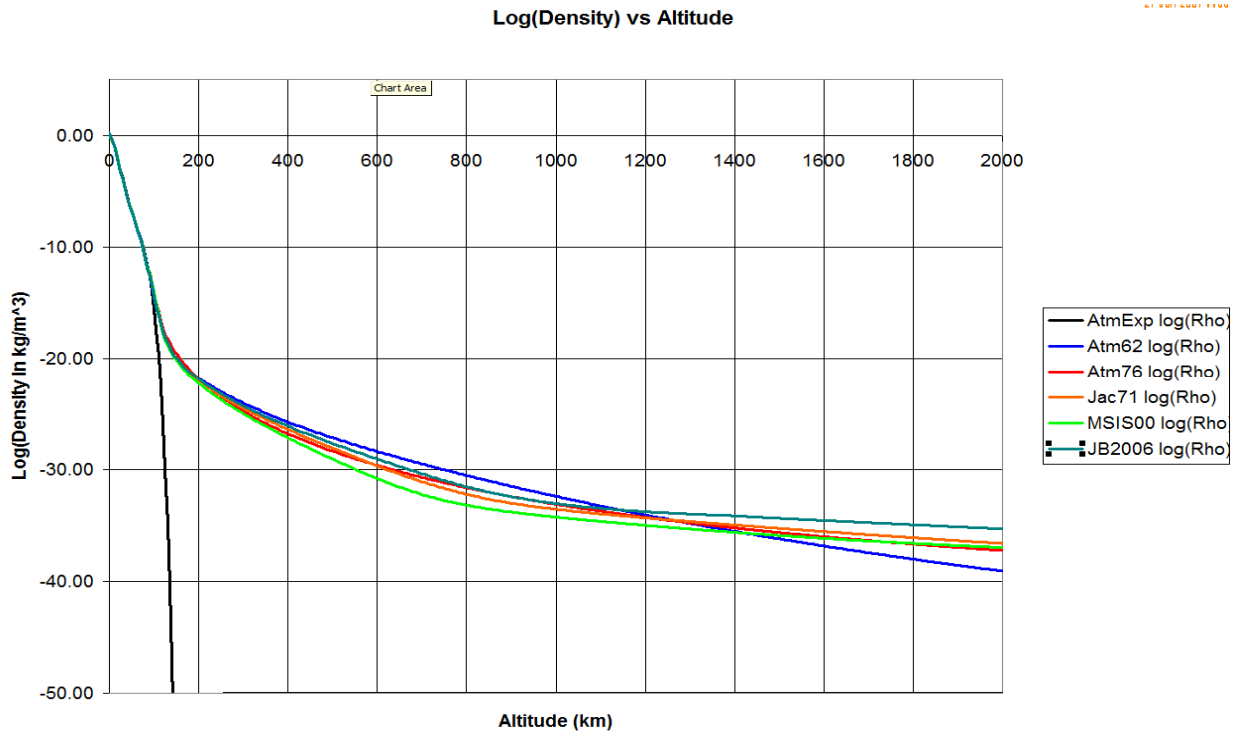
Figure 4. Comparison of a small sampling of atmosphere models.

8.2 Long-Term Solar Flux and Geomagnetic Index Prediction

The goal of the standard is to help minimize space object overpopulation for objects in the LEO-crossing orbit regimes. This is accomplished by standardizing on an anticipated post-mission lifetime of 25 years or less. Utilization of the higher-fidelity atmosphere models mentioned in the previous section requires the orbit analyst to specify the solar and geomagnetic indices required by such models. As can be seen by the careful comparison of Figures 5 through 8, attempts to 'generalize' or abstract solar indices are fraught with error, since they do not capture the true upper and lower variations. Also, note that the "estimated" values from typical solar cycle predictions appear to be located at the mean value of the upper and lower curves. But as shown in Figure 6, the frequency of occurrence is highest near the lowest prediction boundary.

There are other problems with the use of the F10.7 curves shown in Figure 5, notably that the timing of the cycle minima and maxima are always imprecise. The resultant time bias that such a prediction error would introduce could easily yield large F10.7 prediction errors of 100% or more.

The long time duration currently being advocated by the IADC (25 years, although this is still under review) suggests a different approach for the standard. Rather than attempt to predict a 'mean' curve, which would ignore the highly nonlinear aspects of solar storms and quiet periods, the adopted approach is to utilize historical $F_{10.7}$ and A_p (geomagnetic) data[14, 15] directly, thereby retaining the wide variability and nonlinearity of the data. Care is taken to adopt the adjusted $F_{10.7}$ values (adjusted to correct for Earth-sun distance variations). Note that we already have more than five solar cycles of data to choose from. Processing of this data maps each coupled and correlated triad of datum ($F_{10.7}$, $F_{10.7}$ Bar, and A_p) into a single solar cycle range of 10.82546 years (3954 days).

Implementation of this historical data, mapped into a single solar cycle (Figures 9 through 11), then uses random draws upon the number of data triads available on any day within the single solar cycle. Since we have accumulated daily data since 14 February 1947, on any given day within the 3954-day solar cycle we have at least five data triads to choose from. It is important that the random draw retain the integrity of each data triad, since $F_{10.7}$, $F_{10.7}$ Bar, and A_p are interrelated.

In summary, the selected method used in the QPROP analysis tool for modeling solar and geomagnetic data is to select a new coupled triad of ($F_{10.7}$, $F_{10.7}$ Bar, and A_p) data for each day of the orbit lifetime simulation, thereby simulating the drag effect resulting from solar and geomagnetic variations consistent with historical trends for these data. The C++ code that QPROP uses to implement this atmospheric variation strategy has been made publicly available so that users of the proposed orbit lifetime standard can adopt a standardized $F_{10.7}$, $F_{10.7}$ Bar, and A_p prediction if desired.
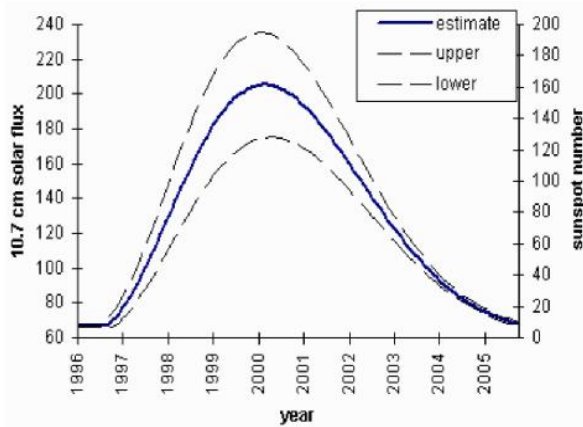
Figure 5. Solar flux estimated upper, lower and mean.   Figure 6. Distribution of F10.7 deviates.
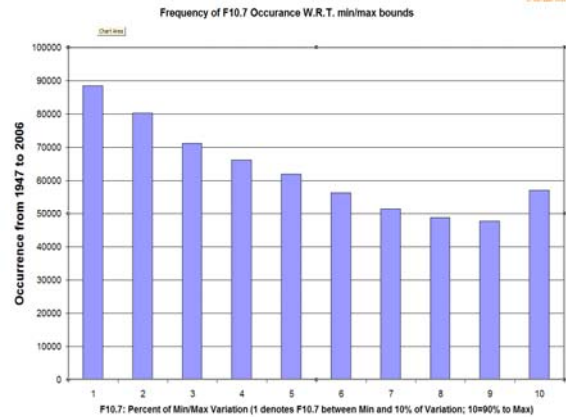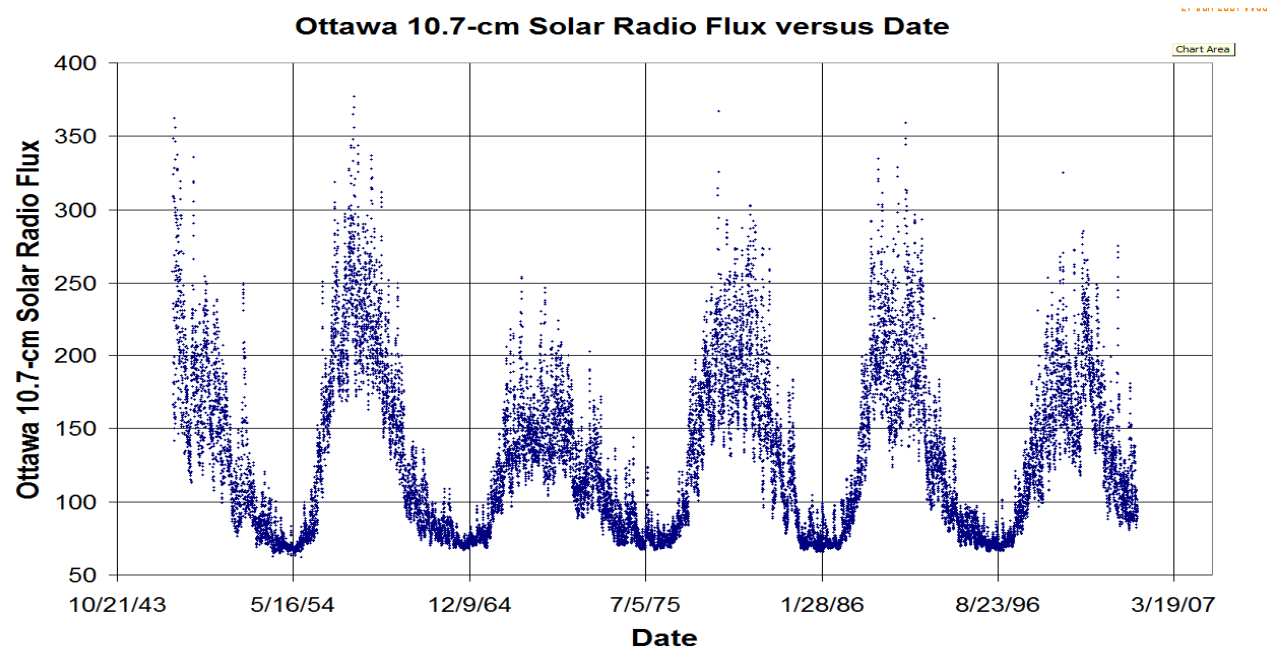
Figure 7. F10.7 Solar data.
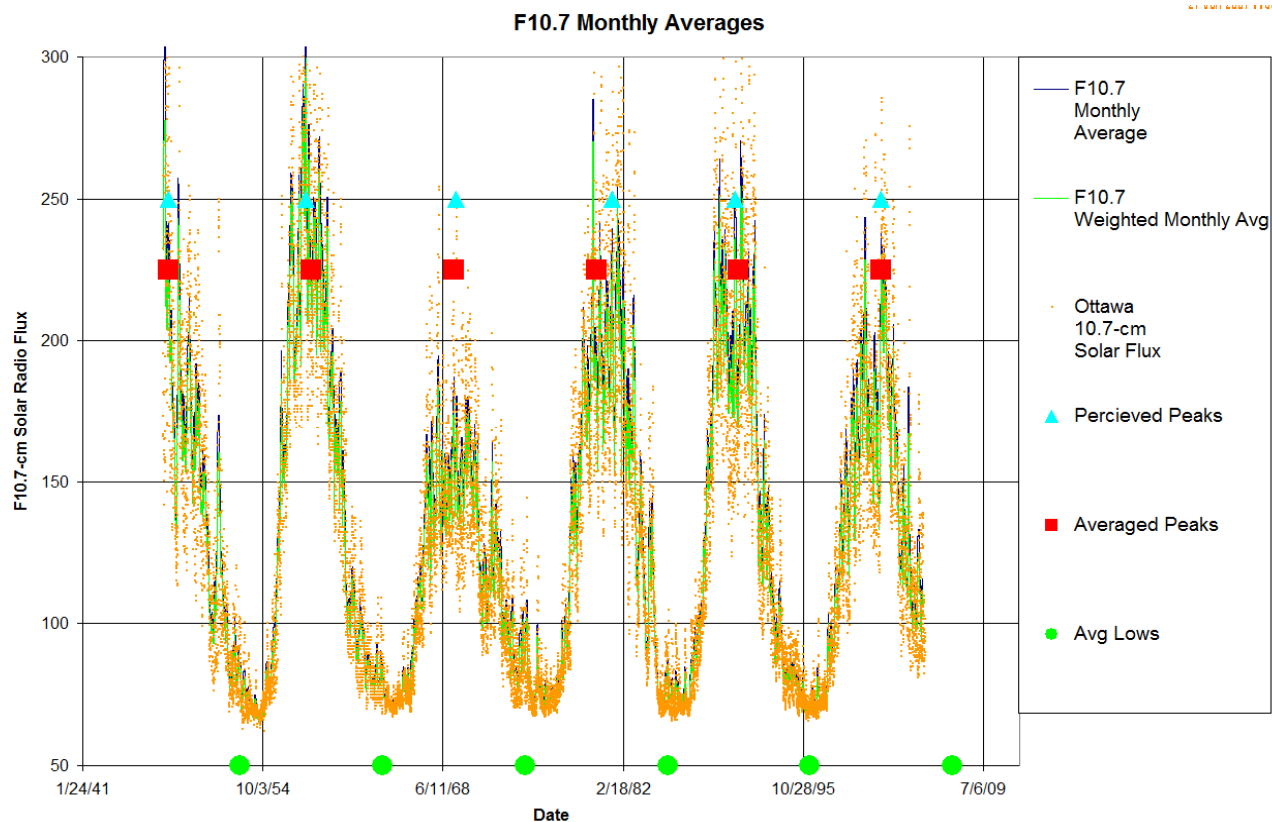
Figure 8. Averaged F10.7 Solar data with minima & maxima.

10
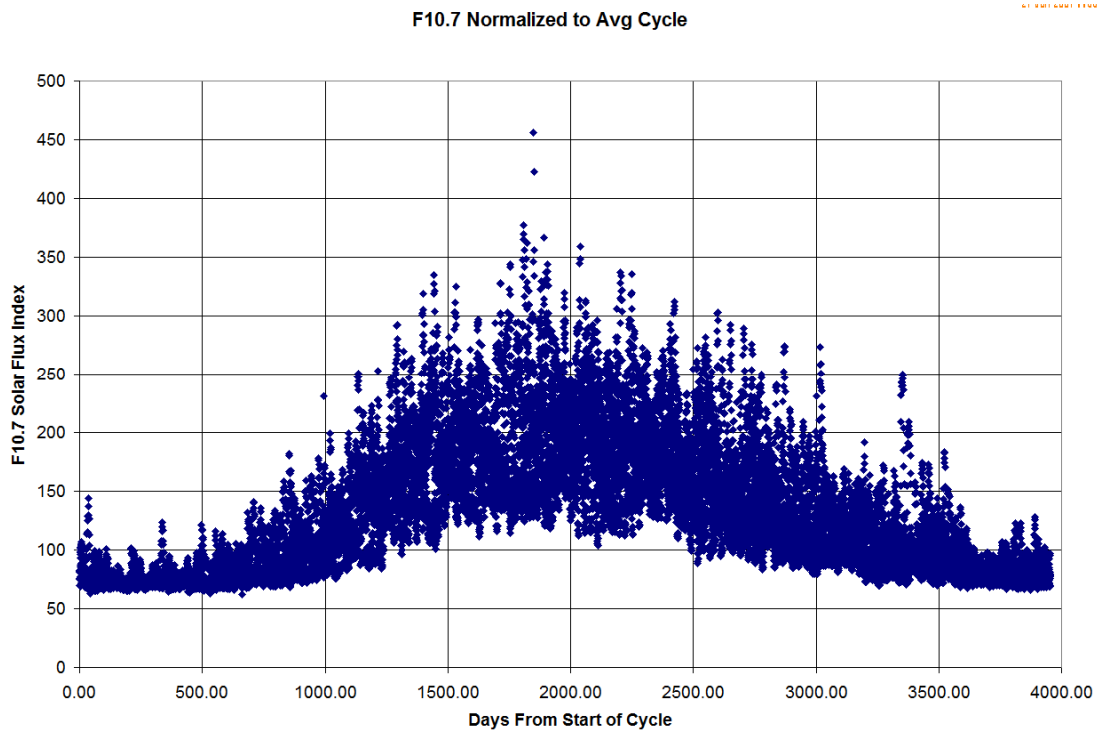
Figure 9. F10.7 Normalized to average cycle.
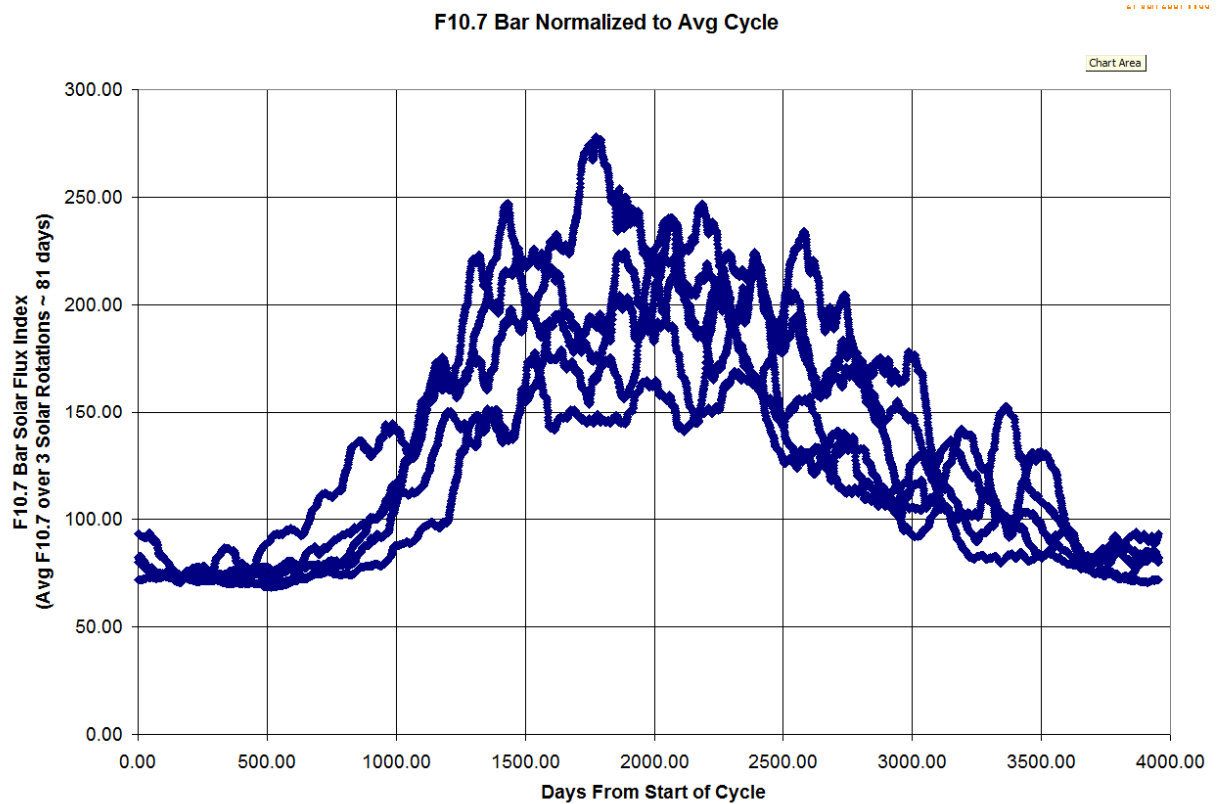
Figure 10. F10.7 Bar normalized to average cycle.

11
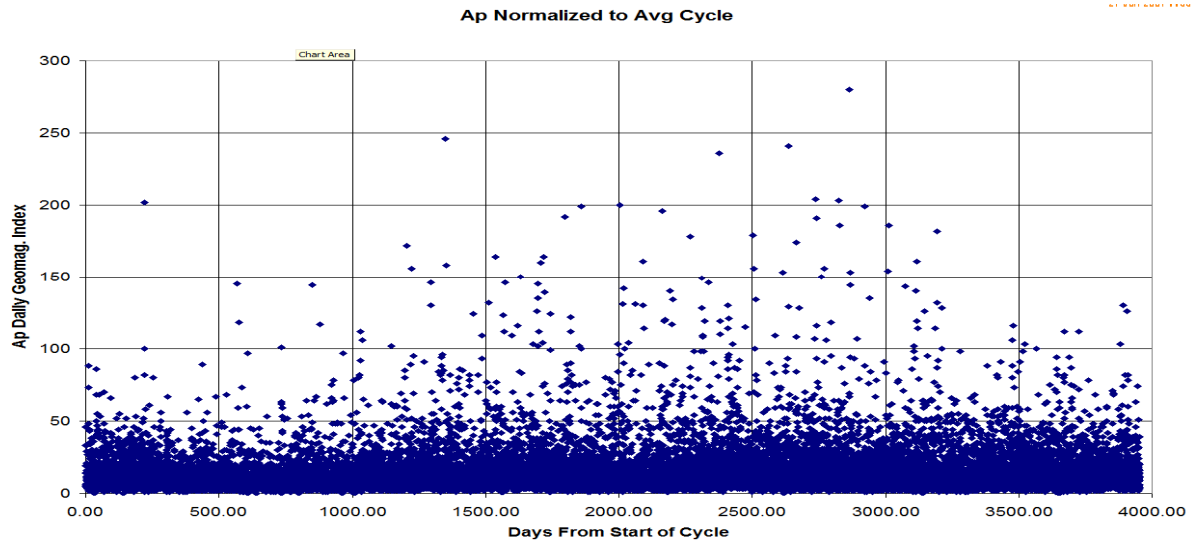
Figure 11. A_p normalized to average cycle.

It can also be seen from Figure 11 that A_p is (1) unpredictable; (2) loosely correlated with the solar cycle; and (3) volatile. Figure 12 demonstrates that density varies greatly depending upon A_p; thus, a geomagnetic storm could induce large decreases in orbital energy (orbit decay) during such storms that the use of some average A_p value would miss. But while this dependency does exist, the unpredictable nature of A_p shown in Figure 11 again illustrates that perhaps the best implementation of geomagnetic index modeling is the use of random draws of historical data, such as we adopt in this report for orbit lifetime standards purposes.
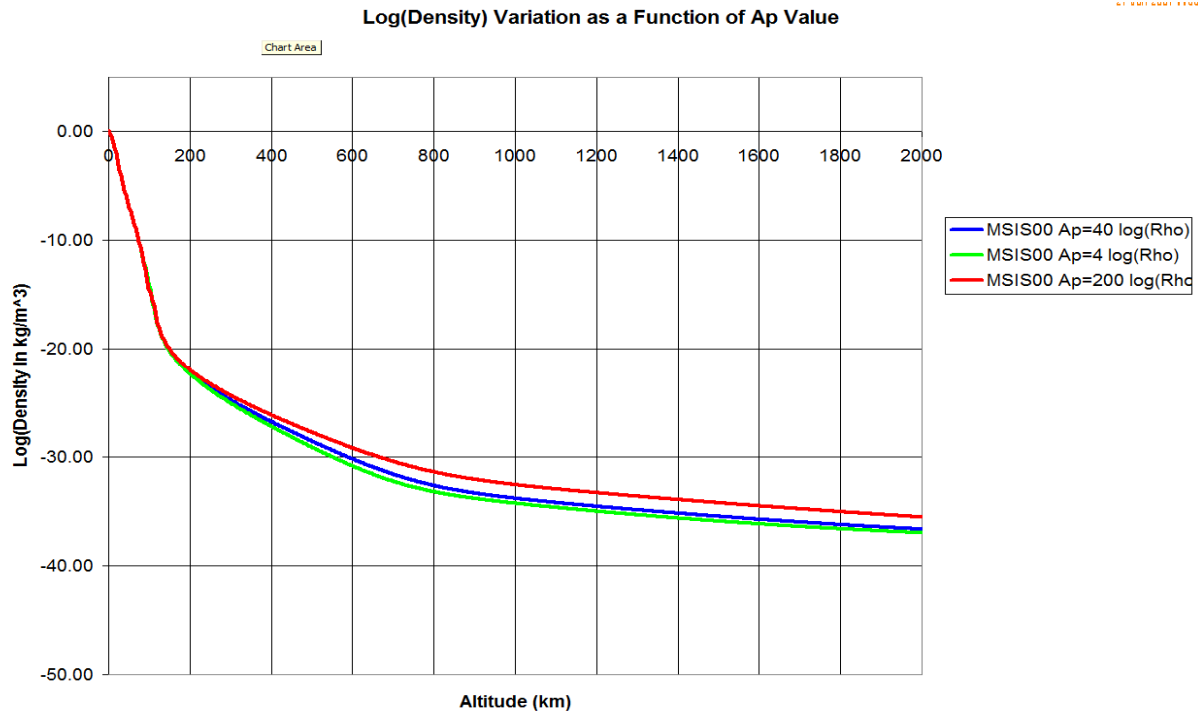
Figure 12. Log (density) variation as a function of A_p value.

12

9. Conclusions

The process of orbit lifetime estimation has been examined, with the goal of standardizing the space community's methods for handling such uncertain parameters as solar and geomagnetic indices, ballistic coefficient prediction, and thermospheric cooling. The two primary methods of assessing orbit lifetime (Methods 2 and 3), together with their derived analysis products (Method 1), provides spacecraft designers, owners, and operators with a variety of assessment methods that span a wide range of orbit initial conditions, implementation effort required, and utility.

Pertaining to the IADC original 25-year guideline for post-mission residency in the 0–2000 km LEO band, numerous computer runs have been accomplished that show the family of post-safing orbit initial conditions that were found to exhibit a 25-year post-mission lifetime. For a user-provided perigee altitude, it is logical that if the user's apogee altitude is below this 25-year proximity region, then the user's post-mission orbit will decay in less than 25 years and will meet IADC guidelines as well as the proposed ISO standard. Conversely, if for the same user-provided perigee altitude the apogee altitude is above the 25-year proximity region, then the user's orbit will not decay within 25 years and therefore violates the IADC guideline and ISO standard. Finally, if the user's specified orbit falls within the region of the 25-year constraint, then it may or may not be an issue; perhaps using increased modeling fidelity (e.g., switching to Method 3, coupled with the statistical solar and geomagnetic indices) would allow the analyst to make a better determination as to whether the IADC guideline and ISO standard requirements will be met.

10. References

1. The U.S. Government Orbital Debris Mitigation Standard Practices may be found on the NASA Orbital Debris Program Office website at http://orbitaldebris.jsc.nasa.gov/library/USG_OD_Standard_Practices.pdf.

2. "IADC Space Debris Mitigation Guidelines," IADC-0201, dated 15 October 2005, URL: http://www.iadc-online.org/docs_pub/IADC-101502.Mit.Guidelines.pdf [cited 25 June 2007].

3. Peterson, G. E., "Optimal Eccentricity Vector for Disposal of Low and Medium Earth Orbiting Satellites," AIAA-2006-6752, AIAA/AAS Astrodynamics Specialist Conference, Keystone, Colorado, 21-24 August 2006.

4.   Kozai, Y., "The Motion of a Close Earth Satellite," *Astronomical Journal* 64, 367—377, November 1959

5.   Roy, A.E., *Orbital Motion*, 2nd ed., Adam Hilger, Ltd, Bristol, ISBN 0-85274-462-5.

6.   Chao, C. C. and Platt, M. H., "An Accurate and Efficient Tool for Orbit Lifetime Predictions," AAS/AIAA Paper 91-134, Feb. 1991.

7.   Liu, J. J. F., and Alford, R. L., "Semianalytic Theory for a Closed-Earth Artificial Satellite," *Journal of Guidance and Control*, Vol. 3, No. 4, 1980, 304-311.

8.   Chao, C.C., Strizzi, J.D. and Oltrogge, D.L., Johnson, C.J., and Williams, S.D., "Improved Reentry Impact Point Prediction Using NORAD Elements and the LIFETIME program," Paper AAS 94-159, AAS Space Flight Mechanics Conference, Cocoa Beach, Florida, February 1994.

9.   *Guide to Reference and Standard Atmosphere Models,* ANSI/AIAA Document #G-003B-2004.

10. Jacchia, L. G. (1971) "Revised Static Models of the Thermosphere and Exosphere with Empirical Temperature Profiles," SAO Special Report No. 332, 1971.

11. Picone, J. M., A. E. Hedin, D. P. Drob, and A. C. Aikin, NRLMSISE-00 empirical model of the atmosphere: Statistical comparisons and scientific issues, *J. Geophys. Res., 107(A12)*, 1468, doi 10.1029/2002JA009430, 2002..

12. Bowman, B. R., Tobiska, W. K., and Marcos, F. A., "A New Empirical Thermospheric Density Model JB2006 Using New Solar Indices," *AIAA 2006-6166, AIAA/AAS Astrodynamics Specialist Conference*, Keystone, CO, August, 2006.

13. Marcos, F. A., "Accuracy of Atmospheric Drag Models at Low Satellite Altitudes," *Adv. Space Res*. Vol. 10, (3), 1990.

14. "2800 MHz SOLAR FLUX," dated 20 October 2006, URL: ftp://ftp.ngdc.noaa.gov/STP/SOLAR_DATA/ SOLAR_RADIO/FLUX/read.me [cited 14 March 2007].

15. "Gottingen Kp/Ap values," dated 20 October 2006, URL: ftp://ftp.ngdc.noaa.gov/STP/GEOMAGNETIC_DATA/ INDICES/KP_AP/read-me.txt [cited 14 March 2007].

16. Ginsberg, L. J. and Luders, R. D., "Orbit Planner's Handbook," The Aerospace Corporation internal report.

17. Cook, G. E., "Satellite Drag Coefficients," *Planetary Space Sciences*, Vol. 13, pp. 929 to 946, 1965, Pergamon Press Ltd. Printed in Northern Ireland.

18. Larson, W. J. and Wertz, J. R. (editors), Space Mission Analysis and Design, 3rd Edition, Space Technology Library, Kluwer Academic Publishers, 2005..

19. Bowman, B. R. and Moe, K., "Drag Coefficient Variability at 175-500 km from Orbit Decay Analyses of Spheres," AAS Paper 05-257, AAS/AIAA Astrodynamics Specialist Conference, Lake Tahoe, CA, August 2005.

20. Bowman, B. R. and Storz, M. F., "High Accuracy Satellite Drag Model (HASDM) Review, AAS 2003-625, AAS/AIAA Astrodynamics Specialist Conference, Big Sky, Mt., August 2003.

21. Marcos, F. A., "Requirements for Improved Thermospheric Neutral Density Models," AAS Paper 85-312, AAS Publications Office, P.O. Box 28130, San Diego, CA 92128, 1985.

22. Chao, C. C., Gunning, G. R., Moe, K., Chastain and Settecerri, T. J., "An Evaluation of Jacchia 71 and MSIS90 Atmosphere Models with NASA ODERACS Decay Data," *Journal of the Astronautical Sciences*, Vol. 45, No. 2, April-June 1997, pp. 131-141.

23. Owens, J. K., "NASA Marshall Engineering Thermosphere Model, Version 2.0, NASA/TM-2002-211786, Marshall Space Flight Center, MSFC, AL, 2002.

24. Wise, J. O., Marcos, F. A., Kendra, M., Bass, J. and Bowman, B., "A Statistical Evaluation of the MET Model for Total Density Prediction," AIAA Paper 2003-569, August 2003.

25. Bowman, B. R., "The Semiannual Thermospheric Density Variation from 1970 to 2002 Between 200-1199 km," AAS 2004-174, AAS/AIAA Spaceflight Mechanics Meeting, Maui, HI, February 2004.

26. Moe, K. and Moe, M.M., "Gas-Surface Interactions and Satellite Drag Coefficients," *Planetary and Space Science* 53 (2005), pp. 793-801, Publisher Elsevier.

27. Meyer, K. W. and Chao, C. C., "Atmospheric Reentry Disposal for Low-Altitude Spacecraft," *Journal of Spacecraft and Rockets*, Vol. 37, No. 5, September-October 2000, 670-674.

28. Marcos, F.A., Wise, J.O., Kendra, M.J., Gossbard, N.J., and Bowman, B.R.., "Detection of a long-term decrease in thermospheric neutral density," *Geophysical Research Letters*, Vol. 32, L04103, doi:10.1029/2004GL021269, 2005.

29. Qian, Liying, Roble, Raymond G., Solomon, Stanley C., and Kane, Timothy J., "Calculated and Observed Climate Change in the Thermosphere, and a Prediction for Solar Cycle 24," *Geophysical Research Letters*, Vol. 33, L23705, doi:10.1029/2006GL027185, 2006.

30. Solomon, Stanley C., Qian, Liying, and Roble, Raymond G., "Thermospheric Global Change during Solar Cycle 24," AGU Fall Meeting, San Francisco, CA, 12 December 2006.

Appendix A: Estimating Ballistic Coefficient (C_DA/m) Considering Tumbling

The first step in planning for a LEO or HEO spacecraft disposal is to estimate the ballistic coefficient (C_DA/m). Cross-sectional area and drag coefficient estimations are examined separately. The spacecraft mass is typically assumed to be constant from EOL until orbit decay.

A.1 Estimating Cross-Sectional Area with Tumbling and Stabilization

The average cross-sectional area should be used to compute the ballistic coefficient of a tumbling spacecraft. This can be as simple as a straightforward two-point average of the minimum and maximum cross-sectional areas, or this approach can be extensively refined by integrating the cross-sectional area of the spacecraft across all anticipated tumbling attitudes, and then dividing the result by the difference between the limits of integration. The analyst is then left with a properly weighted average cross-sectional area. For satellites with a large length-to-diameter ratio, the analyst should consider whether gravity gradient stabilization will occur and adjust the cross-sectional area accordingly. Similarly, for satellites that have a large aero-torque moment (i.e., the center-of-gravity and center-of-pressure are suitably far apart and the aerodynamic force is suitably large), the analyst should consider whether the satellite would experience drag-induced passive attitude stabilization and adjust the cross-sectional area accordingly.

A.2 Estimating Drag Coefficient

The proper value of the dimensionless drag coefficient, C_D, is 2 for a typical spacecraft.

The atmospheric drag force is directly proportional to the ballistic coefficient, C_DA/m, contained in the equations of motion. The drag coefficient, C_D, depends on the shape of the satellite and the way air molecules collide with it. In free molecular flow, C_D is usually assumed to be the theoretical value of 2. However, for certain geometric configurations such as spheres, cylinders and cones, the value of axial drag coefficient, C_D, can be evaluated more precisely than previously noted provided something is known about the flow regime and reference area.

As discussed in Ref. 16, the atmosphere above 150 km can be represented by free molecular flow conditions. The free molecular flow regime is defined by the Knudsen number, K_n, which is the ratio of the mean free path of a molecule to some reference length of the body pertinent to the flow field. For example, the mean free path at 150 km altitude is about 6.5 m. Therefore, for a 1.6-m diameter spacecraft, the Knudson number is about 4, which is in the transition-to-free-molecular flow region. The drag coefficient of simple symmetrical bodies, such as spheres, cylinders and cones, may be analytically expressed[18] as a function of spacecraft to molecule speed ratio s:

$$s = V / v_{mp} \tag{A-1}$$

where V is the spacecraft's velocity and v_{mp} is the most probable molecular speed. The mean molecular speed, v*, is given in most atmospheric tables such as ARDC 1959 and can be corrected to given v_{mp} as follows:

$$v_{mp} = 0.8862\ v^* \tag{A-2}$$

For example, assume a satellite is at 555 km with a velocity of about 7.6 km/sec. The most probable molecular speed is about 1.19 km/sec. Thus, the molecular speed ratio s is about 6.4. At 740 km

altitude, s = 5.9. Figure A-1 gives the drag coefficients for a sphere for both diffuse and specular reflection[16] (i.e., angle of incidence equals angle of reflection). For design or analysis purposes, curves for diffuse reflection should be used, since the fraction of diffusely-reflected particles is quite high for free molecular flow. Figure A-2 gives drag coefficients for a cylinder[16].

Note that for high molecular speed ratios, $C_D \cong 2$ is reached for spherical bodies and $C_D \cong 3$ for cylindrical bodies with the relative wind along the axis of rotation of the cylinder. These values are quite adequate as a first approximation. For speed ratios much lower than 5 for spherical bodies or much lower than 2 for cylindrical bodies, the above approximation is no longer good, as shown in Figures A-1 and A-2. For example, in the LIFETIME program the C_D value is computed from an empirical equation as a function of altitude determined from Newtonian flow when the altitude is lower than 125 km. A theoretical discussion[17] of drag coefficients in 1965 also supports the above approximation ($C_D \cong 2.2$ for spheres).
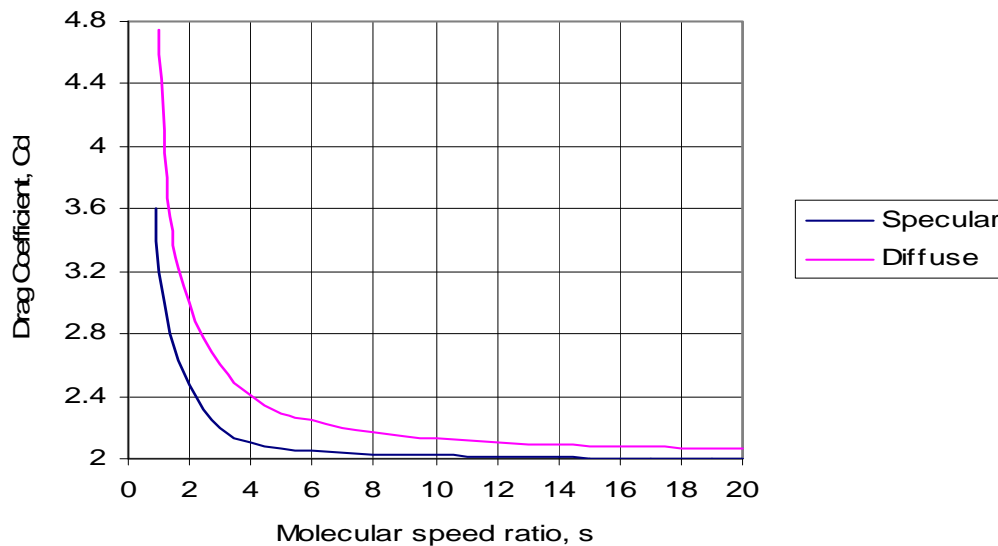
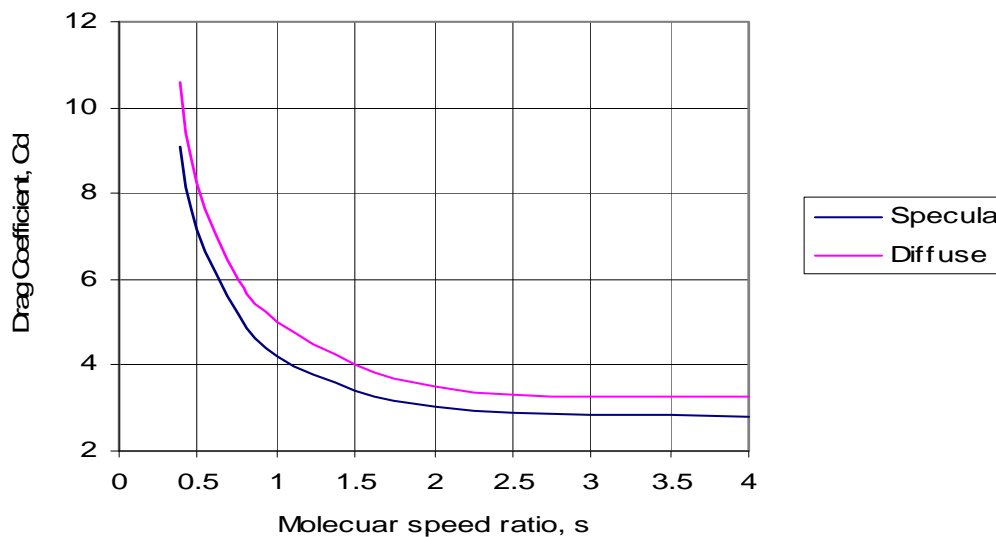Figure A-1. Sphere drag coefficient, diffuse and specular reflection.

Figure A-2. Cylinder drag coefficient, diffuse and specular reflection.

17

Based on the approximate mass, shape, size and orientation of various LEO satellites, values of ballistic coefficients and drag coefficients were estimated from post-flight orbit determination.[18] The typical upper and lower limits of drag coefficients are 4 and 2, respectively.[18] Table A-1 shows the maximum and minimum values of the 16 satellites in low Earth orbit. The estimated drag coefficients are bounded between 2 and 4.

Table A-1. Estimated Ranges of Drag Coefficients for Low-Earth Orbit Satellites*

Satellite	Mass, kg	Shape	Max XA (m^2)	Min XA (m^2)	Max XA C_D	Min XA C_D	Type of mission
Oscar-1	5	box	0.075	0.0584	4	2	Comm.
Intercos-16	550	cylinder	2.7	3.16	2.67	2.1	Scientific
Viking	277	octagon	2.25	0.833	4	2.6	Scientific
Explorer-11	37	octagon	0.18	0.07	2.83	2.6	Astronomy
Explorer-17	188.2	sphere	0.621	0.621	2	2	Scientific
Sp. Teles.	11,000	cylinder	112	14.3	3.33	4	Astronomy
OSO-7	634	9-sided	1.05	0.5	3.67	2.9	Solar Phys
OSO-8	1,063	cylinder	5.99	1.81	3.76	4	Solar Phys
Pegasus-3	10,500	cylinder	264	14.5	3.3	4	Scientific
LandSat-1	891	cylinder	10.4	1.81	3.4	4	Rem Sens
ERS-1	2,160	box	45.1	4	4	4	Rem Sens
LDEF-1	9,695	12-face	39	14.3	2.67	4	Environm
HEAO-2	3,150	hexagon	13.9	4.52	2.83	4	Astronomy
Vanguard-2	9.39	sphere	0.2	0.2	2	2	Scientific
SkyLab	76,136	cylinder	462	46.4	3.5	4	Scientific
Echo-1	75.3	sphere	731	731	2	2	Comm.

*Courtesy of J. Wertz of Microcosm.

A.3 Recent Studies

According to Bowman and Moe,[19] the US Air Force has long supported efforts to improve satellite orbital predictions, in cooperation with the US Navy, NASA, the Harvard-Smithsonian Center for Astrophysics, and many universities and Air Force contractors. Over the years, Air Force prediction efforts have evolved along two lines:

- In the High Accuracy Satellite Drag Model (HASDM)[20] program, many orbiting satellites are used to monitor the atmosphere and update an atmospheric model in real time

- In the DMSP program, the spectroscopic sensors SSUSI and SSULI will monitor the atmosphere and update it.

A major objective of both these programs is to measure and predict absolute atmospheric densities. Improvement in the knowledge of drag coefficients contributes directly to that goal.

Better drag coefficients also contribute to the improvement of thermospheric density models. A landmark in the effort to improve density models was achieved by Marcos[21] in 1985 when he compared and evaluated 14 models against accelerometer measurements from seven satellites. A decade later, Chao et al.[22] used orbital data from the ODERACS I and ODERACS II families of spheres to measure the biases in the Jacchia 71 and the MSIS 90 density models near sunspot

minimum. They accomplished this by comparing the fitted drag coefficient, C_D, with the physical drag coefficient, C_{DP}, calculated from the actual momentum transfer to the satellite. Results of their study indicated that the C_{DP} values range from 2.08 to 2.3 for altitudes between 150 km and 350 km. Their results also show that MSIS90 model yields a more accurate prediction of atmospheric density in that altitude region. More recently, Owens[23] has revised and improved the Jacchia models to create the NASA Marshall Engineering Thermospheric Model –Version 2.0 (MET-V 2.0 Model). This model has been subjected to an extensive statistical evaluation by Wise et al.[24] Further recent progress by Bowman[25] in the analysis of orbital data has refined the semiannual variation and other parameters of the Jacchia 70 thermospheric density model.[10] This new development presented an opportunity to use the improved Jacchia model with data from spherical satellites to refine our knowledge of drag coefficients and improve the absolute densities in the model.

In 2005, Bowman and Moe[19] applied density corrections to the improved Jacchia model with tracking data from numerous spherical satellites to compute accurate fitted drag coefficients. Furthermore, they calculated physical drag coefficients from parameters of gas-surface interaction previously measured in orbit. Jacchia originally assumed that the physical drag coefficient of compact satellites is 2.2 at all altitudes. Comparison of the two types of drag coefficients has made it possible to remove from the atmospheric model the bias that this assumption causes.

Based on the findings of Bowman and Moe, the drag coefficient, C_D, of 2.0 should be used with the Jacchia-Bowman JB2006 model for computing satellite orbit decay and lifetime. This newest density model considers the C_D variation as a function of altitude. For spacecraft shape significantly different from a sphere, such as a cylinder with the relative wind along the axis of rotation, a C_D value of 3 may be used. A recent paper by Moe[26] gives the estimated ranges of C_D for spheres and cylinders as a function of altitude and percentage of diffuse reflection.

Appendix B: 25-Year Lifetime Predictions Using Random Draw Approach

Approaches have been developed by the authors that implement the solar and geomagnetic modeling techniques presented in Section 6.2 of this paper.   In this first approach, the 1Earth Research semi-analytic orbit propagator 'QPROP' was used to examine the 7.68 million cases contained in Table B-1. Each one of these cases exhibits the type of orbital lifetime decay shown in Figure B-1.
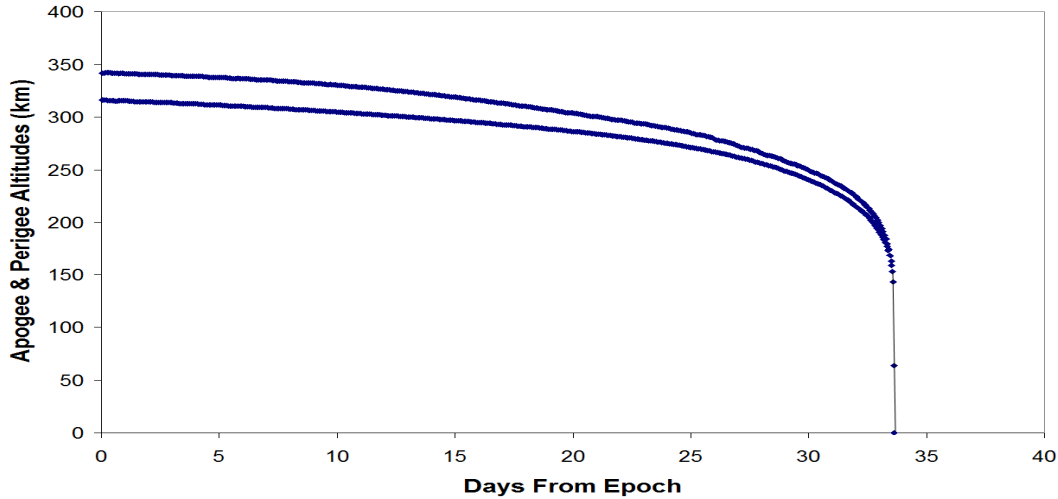

Figure B-1. Sample orbital decay profile of apogee and perigee altitudes versus time.

For a satellite having a ballistic coefficient of 200 cm^2/kg and starting in a circular, equatorial orbit at the altitude shown, Figure B-2 depicts the resultant ranges of anticipated orbit lifetime. The 'minimum' and 'maximum' incorporates the entire range of orbit decay start times with respect to the solar cycle minimum. The right-hand side of the plot shows how variable the results can get in the neighborhood of 25 years' estimated lifetime.

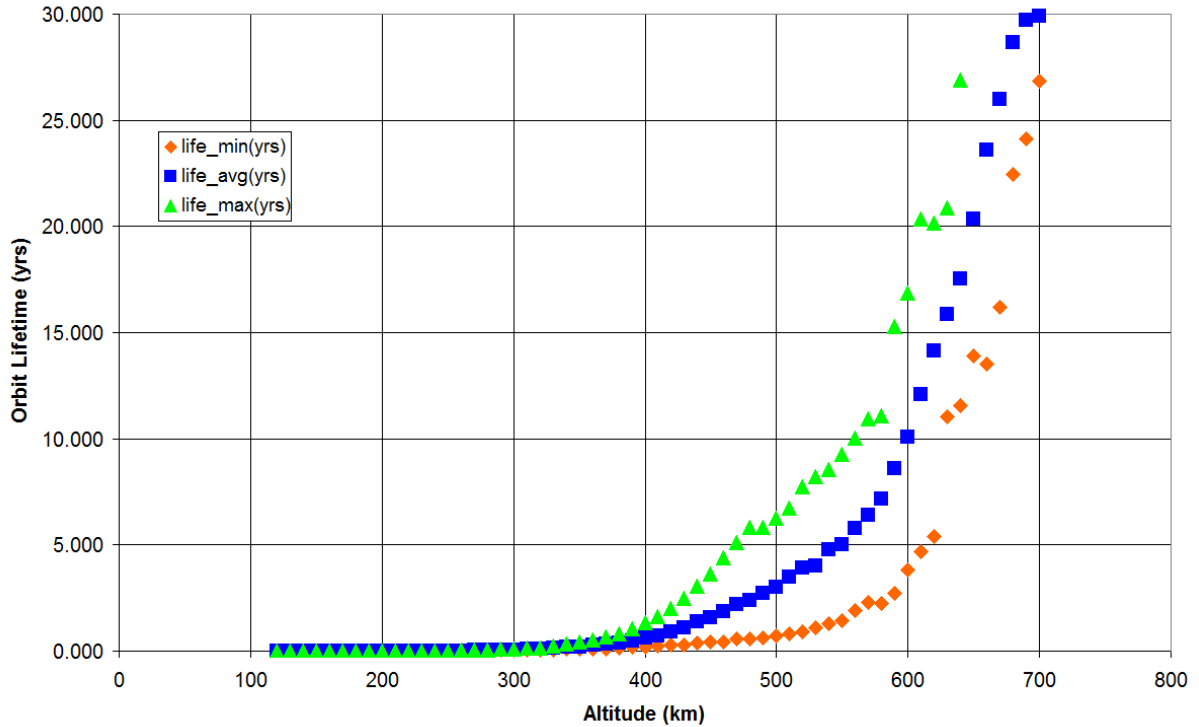## Orbit Lifetime vs Initial Circ Orbit Altitude
(CdA/m=200 cm^2/kg; Equatorial Orbit)

Figure B-2. Sample: orbit lifetime ($C_DA/m = 200$ cm^2/kg, equatorial orbit) as a function of initial orbit altitude.

The primary independent variables of the orbit lifetime estimation process are contained in Table B-1. The dependence of orbit lifetime upon orbit inclination is shown for the same 200 cm^2/kg sample case in Figure B-3. By stepping through all of these variables in the ranges and step sizes indicated in the table, and then detecting those cases that resulted in a 25-year orbit lifetime, the dependencies between ballistic coefficient and orbit initial condition can be found, as shown in Figures B-4 and B-5. While both the MSISE2000 and JB2006 atmosphere models are implemented in QPROP, the MSISE2006 model was used for these analyses due to its faster runtime with similar long-term propagation accuracy. Random draws of the triad of solar and geomagnetic index parameters (discussed in Section 6.2) were implemented. In order to capture variations exhibited by the random draw process, a number of trials were used (four, in this case).

Table B-1. QPROP Grid of Test Cases

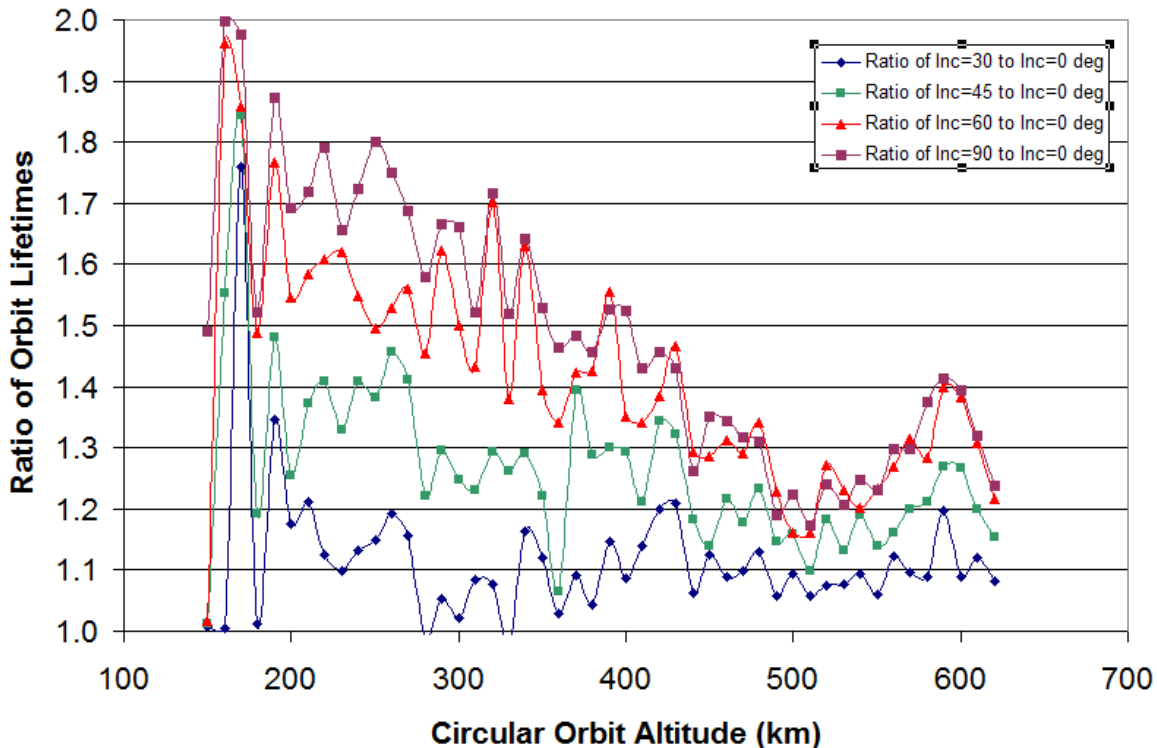| Parameter	Lower Limit	Upper Limit	Step Size
Time into Solar Cycle (days)	0	2964.75	3953/4
Inclination (deg)	0	90	30
C_DA/m	25	500	25.
Perigee Altitude (km)	100	2000	50
Apogee Altitude (km)	250.	10000	50
Number of Trials	0	3	1

21

Figure B-3. Orbit lifetime dependence upon orbit inclination.

Future studies may use more trials and incorporate finer step sizes, but the large computer runtime requirements of these many cases led to the initial selection of four trials per initial set of orbit conditions. Through extensive simulation, it was found for *non-sun-synchronous* orbits that orbit lifetime results are not sensitive to the three angular orbit elements (RAAN, argument of perigee, and mean anomaly) and therefore the three initial values are arbitrarily chosen and assumed for all cases. Note that the sensitivity to RAAN and argument of perigee may be significant for sun-synchronous, Magic, and Molniya orbits; this is discussed in Section 8.1. Note: it is recommended that sun-synchronous orbit cases be studied using a 'Method 2' or '3' approach until such time as their orbit lifetimes can be appropriately categorized in graphical and/or functional form. Further, it was found that orbits having inclinations greater than 90 degrees could be well-represented by the pole-symmetric orbits having complementary orbit inclinations (justifying analysis of only 0 to 90 degrees as shown in Table B-1).

The colored regions shown in Figures B-4 and B-5 denote the categorization of the orbit initial conditions at the start of the orbit decay with respect to the IADC 25-year recommended post-mission lifetime. The 'green' region denotes orbit initial conditions that will result in an orbit lifetime shorter than 25 years (in all observed cases). The 'yellow' region denotes initial orbit conditions that could result in an orbit lifetime that is greater than the recommended 25-year limit in certain circumstances.

One can observe from Figures B-4 and B-5 that there is a wide variety of initial orbit, timing, solar and geomagnetic conditions that can combine to produce an orbit lifetime of 25 years. These figures, while helpful, still leave the user with uncertain knowledge of what the post-mission orbit lifetime will be specific to their initial conditions. Fortunately, the results of the 7.68 million analyses have

22

been retained; interpolation of these results is possible to predict orbit lifetime for a specific set of initial conditions. And, to the extent that four sets of random draw cases is not necessarily an exhaustive analysis, additional cases can be run to further refine the orbit lifetime estimation grid and improve interpolation results.
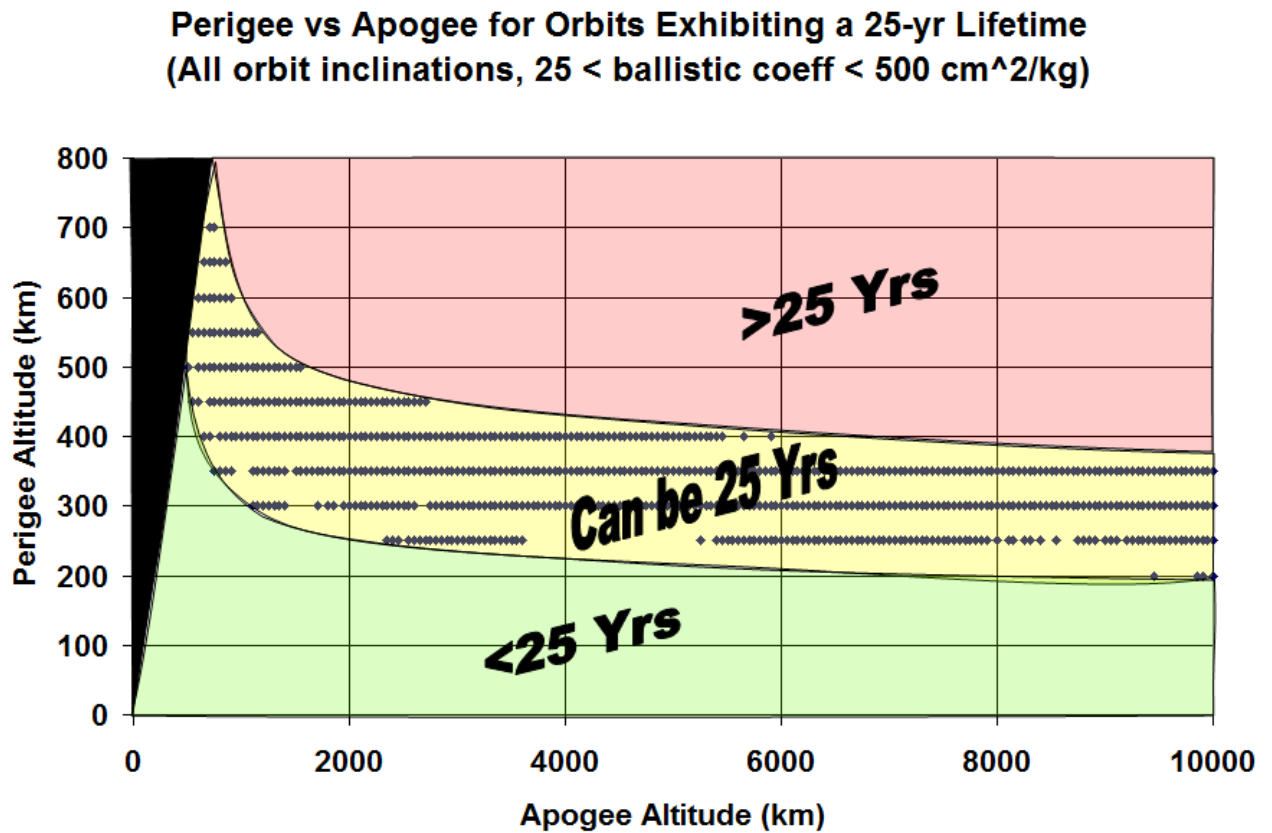
Perigee vs Apogee for Orbits Exhibiting a 25-yr Lifetime (All orbit inclinations, 25 < ballistic coeff < 500 cm^2/kg)

Figure B-4. Perigee versus apogee boundaries for 25-year orbit lifetime conditions ($25 < C_D A/m < 500$ cm^2/kg).
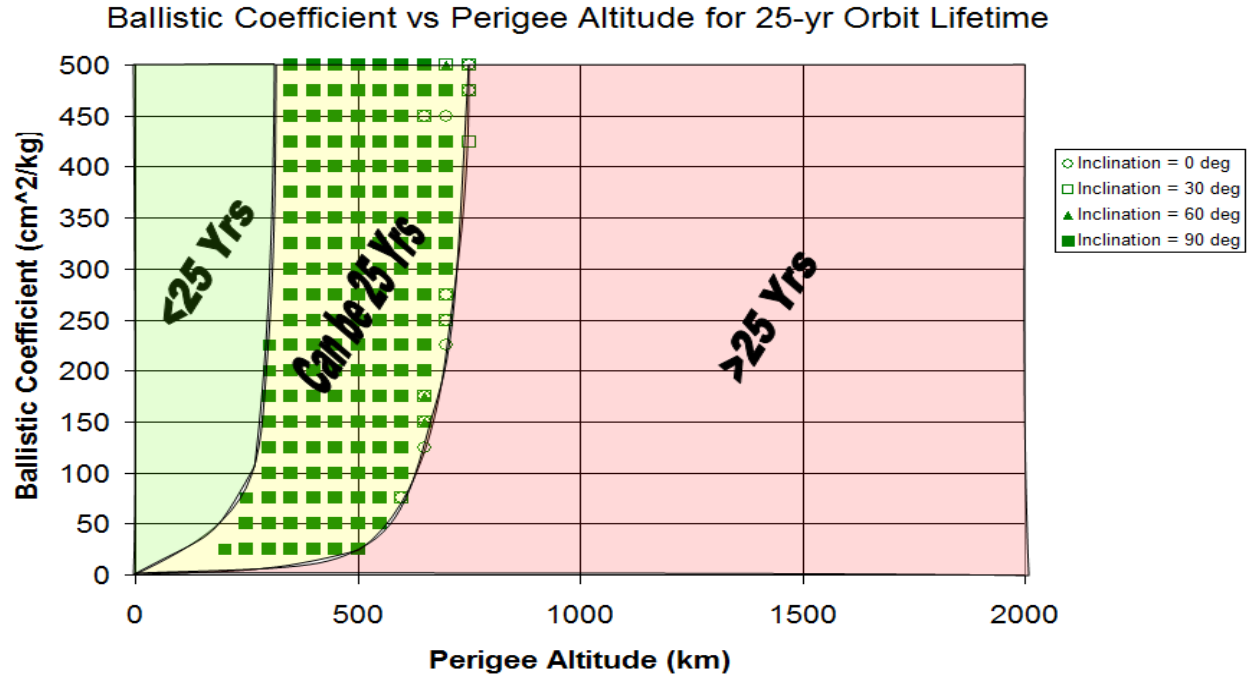
Figure B-5. Ballistic coefficient versus initial perigee altitude for all cases exhibiting 25-year orbit lifetime (apogee assumed < 10,000 km).

A by-product of the many orbit lifetime analysis runs is a set of analytical expressions (Equation B-1) that predict *average* orbit lifetime as a function of H_p, inclination, ballistic coefficient, and orbit eccentricity. The term 'average' denotes orbit lifetime averaged over all historical ranges of solar/geomagnetic indices as well as timing of the initial condition epoch with respect to solar minimum. Although it is difficult to fit analytical expressions to an orbit lifetime that has been averaged over all solar/geomagnetic historical conditions and over the entire range of timings into the solar cycle, a reasonable result has been obtained as shown in Figures B-6 and B-7. Limited step size resolution in H_p, H_a, and time into solar cycle (four points across cycle) further hampered the fit process.

This analytical approximation exhibits a peak deviation of 100% from the underlying estimated lifetime data in extreme cases (Figure B-6), coupled with an average standard deviation of less than 20% error above 200 km (Figure B-7).

Orbit Life(H_p, H_a, β, and inc) = Life(circ alt of H_p) * Factor(H_{avg} , inc) * Factor(β) * Factor(Ecc)

where:

Life(circ alt of H_p) =

- if $H_p < 550$ km: Life(circ alt of H_p) = $F_1 * (H_p \text{ in km})^{F_2}$;

- else: Life(circ alt of Hp) = $F_1 * (H_p \text{ in km})^{F_2} * [1.0 + F_4 * (Hp - F_3)^{F_5}]$ (B-1)

24

Factor (H$_{avg}$, inc) =

- if H$_{avg}$ < 155 km: Factor (H$_{avg}$, inc) = 1.0;

- else if H$_{avg}$ > 550 km: Factor (H$_{avg}$, inc) = 1.3 – 0.00333333 * abs (90 - inc, deg);

- otherwise: Factor (H$_{avg}$, inc) =

  -0.9307 * cos^2 (inc) - 0.2286 * cos (inc) + 2.1011] exp [K * H$_{avg}$],

where: K = (2.E-07 * (90 - inc, deg) ^{2} + 4.E-06 * abs (90 - inc, deg) - 0.0009) if 30 < inc < 150 deg
or K = -1.33333E-06 * (inc, deg) if inc < 30 deg
or K = -1.33333E-06 * (180 - inc, deg) if inc > 150 deg

Factor(β) = [**F$_6$** + **F$_7$** * (β in cm^2/kg) ^{F_8}]

Factor(Ecc) = [1.0 + **F$_9$** * (H$_p$ in km)^2 / (**F$_{10}$** + (H$_p$ in km)^3) * (**F$_{11}$** $^{(F_{12} * Ecc)}$ – 1.0)]

| Coeff	Initially, use:	If Resultant Lifetime < 1 year:
F$_1$	6.350724982689956e-020;	6.350724982689956e-020;
F$_2$	6.295460674885141e+000;	5.946396392270378e+000;
F$_3$	4.820503248857688e+002;	3.185325139041694e+004;
F$_4$	3.919897205867653e-006;	3.137120106945147e+004;
F$_5$	2.367023890310601e+000;	3.137356808942190e+004;
F$_6$	-6.612928883060383e+000;	6.049861647189439e+001;
F$_7$	2.285691478658406e+004;	1.203161061917634e+005;
F$_8$	-8.492321907172038e-001;	-9.158828054010361e-001;
F$_9$	5.303219229102377e+005;	1.522209799457603e+005;
F$_{10}$	-8.474659230907487e+005;	2.718074721276698e+006;
F$_{11}$	1.000349462601627e+000;	1.000780241340044e+000;
F$_{12}$	8.790821659324631e+002;	2.065283320597687e+003;

Fit Percent Error Versus Perigee Altitude
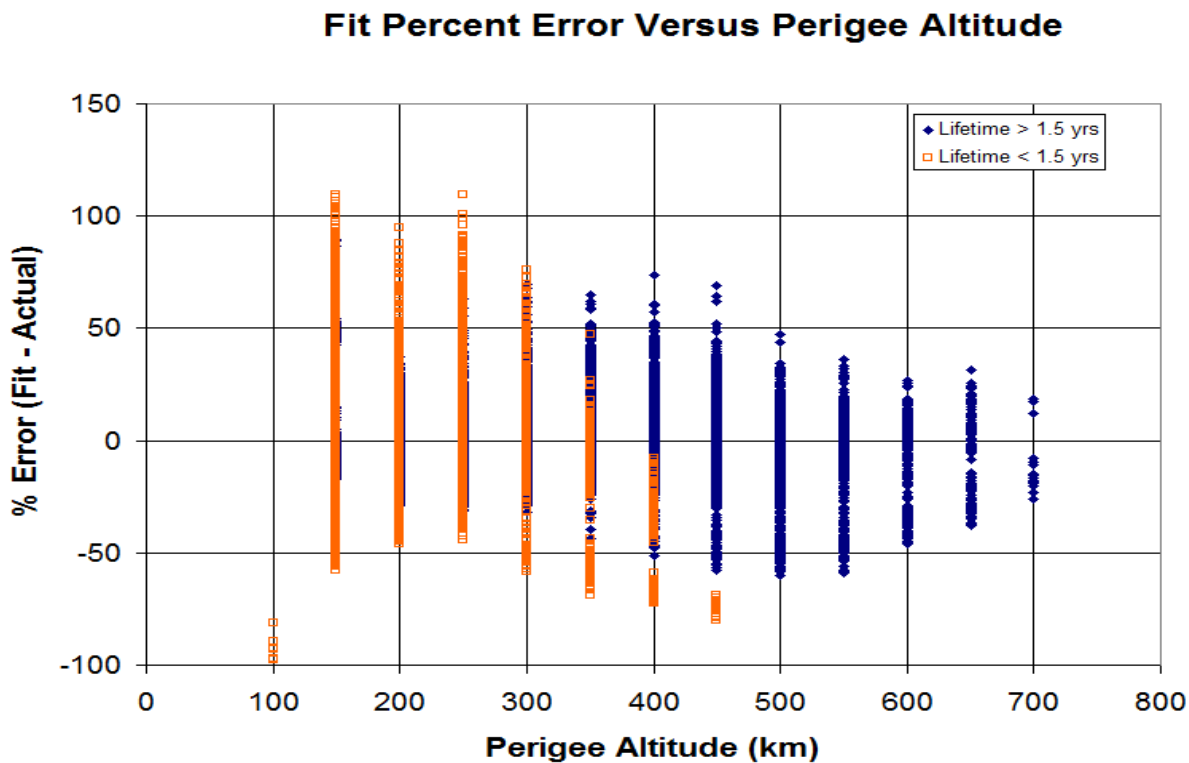
Figure B-6. Percent fit error versus perigee altitude.

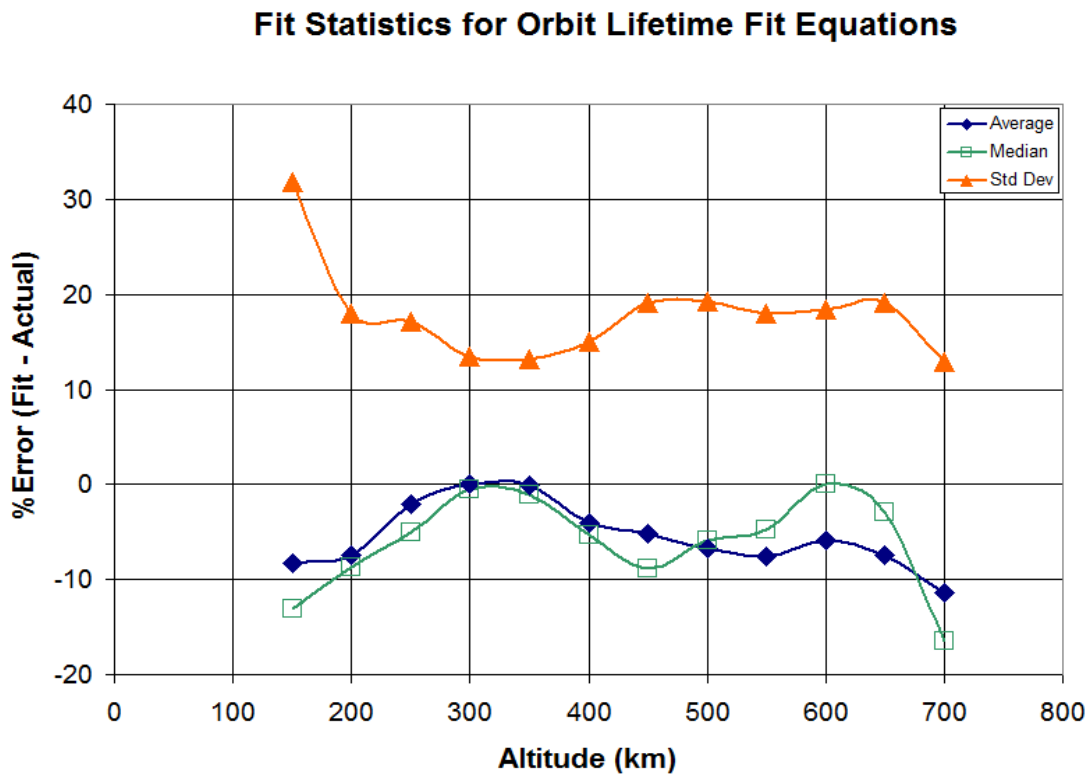## Fit Statistics for Orbit Lifetime Fit Equations

Figure B-7. Fit statistics for orbit lifetime fit equations.

26

Careful examination of Figures B-5 and B-6 shows that polar orbits experience reduced atmospheric drag, due to a polar orbit's reduced time spent under the solar subpoint (where solar heating causes the atmosphere to expand outward into space, thereby causing atmospheric density to rise). Therefore, a highly-inclined orbit requires a higher ballistic coefficient (perhaps an 80 cm^2/kg increase) to match the same 25-year orbit lifetime constraint observed in the low-inclination orbit case for an equivalent combination of perigee and apogee altitudes.

Appendix C: 25-Year Lifetime Predictions Using Median Density Approach

In this approach, the satellite orbit is propagated with a semianalytical tool (LIFETIME) using the Jacchia-Bowman 2006 atmosphere density model (JB2006) based on a 50th percentile solar flux prediction (Figure C-1). The new solar flux indices for the JB2006 model are also the approximated predictions using the same 50th percentile. The fundamental difference of this method is that the F10.7 and A_p values are the predetermined 13-month mean at the 50th percentile, unlike the random draw method based on daily values of several 11-year cycles. The 25-year lifetime is determined by iteration of initial eccentricity holding initial apogee constant. The results of this approach can be used as an independent verification of the random draw approach.

A common epoch of 1 January 2005 is assumed for all the 25-year lifetime propagations. This epoch, which is near the start of the low solar flux period, gives the longest lifetime. Thus, the results of this method are conservative and would ensure that all cases did not exceed the 25-year guideline. The peak-to-valley variation in lifetime due to difference in epoch can be as large as 4.4 years. Similar sensitivity to epoch is reported in an early study by Meyer and Chao.[27]
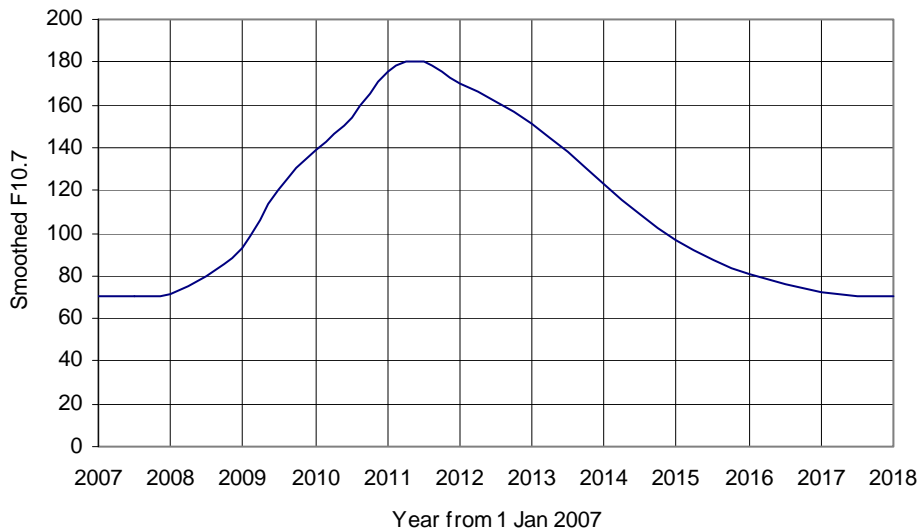

Figure C-1. A 50th percentile of 13-month mean solar flux ($F_{10.7}$).

A large number of 25-year cases were generated based on the following assumed orbit conditions. Again, it was found for non-sun-synchronous orbits that orbit lifetime results are not sensitive to the three angular orbit elements and therefore the three initial values are arbitrarily chosen and assumed for all cases. Note that the sensitivity to RAAN and argument of perigee may be significant for sun-synchronous, Magic and Molniya orbits; this is discussed in Section 8.1.

- Apogee altitude = 500 km to 1200 km at 100 km step
- Ballistic coefficient = 100, 300, 500 cm^2/kg
- Inclination = 0, 30, 60, 90 deg
- Right ascension of ascending node = 260 deg
- Argument of perigee = 80 deg
- Mean anomaly = 0 deg

28

Figures C-2 and C-3 show the converged solutions for 25-year lifetimes at 90 and 30 deg inclinations, respectively. The tolerance for a converged solution is when the lifetime is within +/- 6 months of 25 years. It is interesting to see that the three curves for the three values of ballistic coefficient are nearly linear for apogee altitude higher than 600 km. The well-behaved curves in Figures C-2 and C-3 suggest that the solutions may be more conveniently represented by families of semiempirical equations. A general equation with empirical constants has been derived as:

$$\text{Eccentricity} = C_1(H_a - B_1) - C_2/(H_a - B_2) \tag{C-1}$$

where H_a is initial apogee altitude and the four constants, C_1 B_1 C_2 and B_2, are determined by fitting to each curve in the two figures. The first term in the above equation gives the linear change, while the second term approximates the gradual deviations at low apogee region. The values of these constants for all the above cases are given in Table C-1.
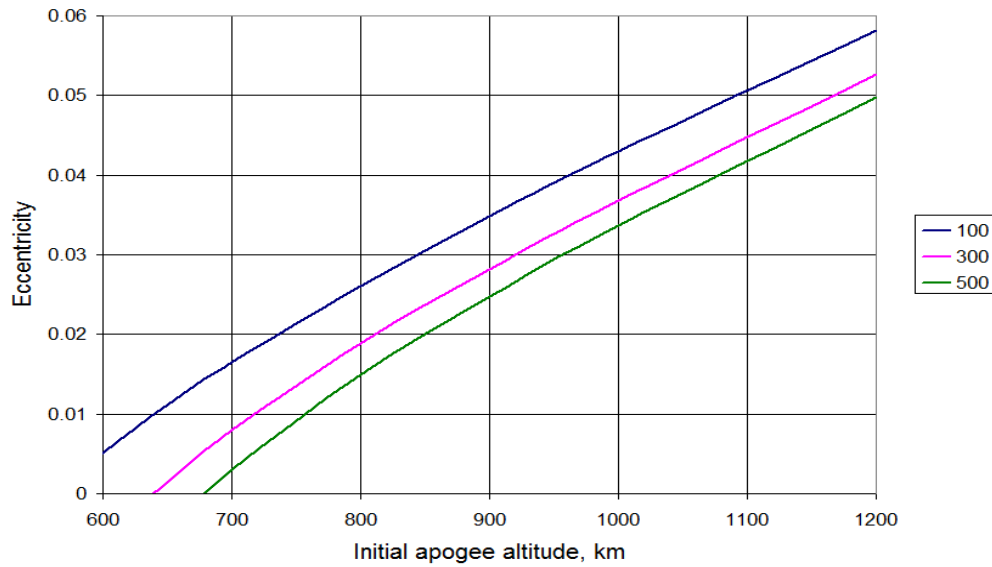

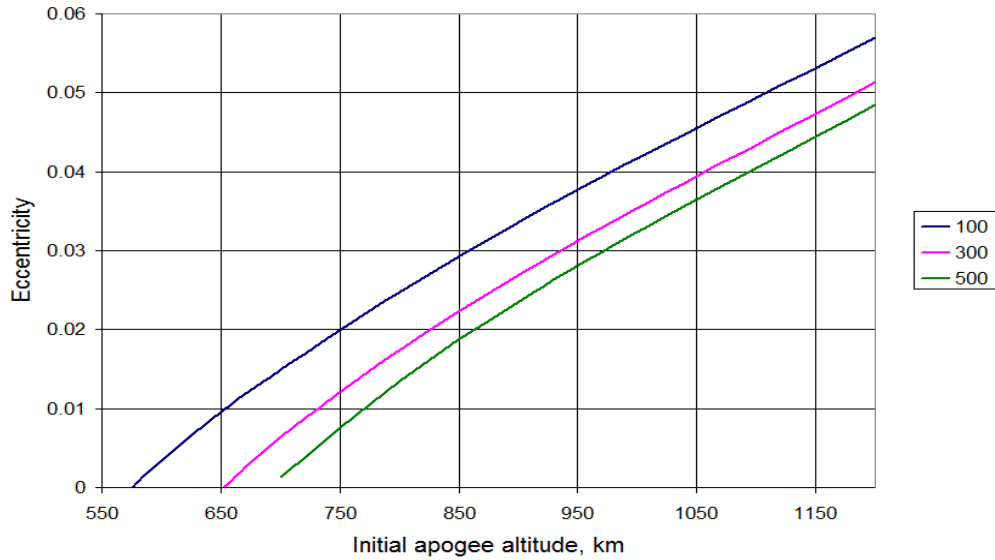Figure C-2. Eccentricity vs. initial apogee altitude for 25-year lifetime at 90 deg inclination with $C_DA/m = 100$, 300 and 500 cm^2/kg.

Figure C-3. Eccentricity vs. initial apogee altitude for 25-life lifetime at 30 deg inclination with $C_DA/m = 100$, 300 and 500 cm^2/kg.

Table C-1. Values of C_1, B_1, C_2 and B_2 for Equation 4

Inclination, deg	C_D A/m, cm^2/kg	C_1	B_1	C_2	B_2
0	100	0.00008	480	0.4	540
	300	same	550	0.65	600
	500	same	580	0.6	640
30	100	0.00008	465	0.42	550
	300	same	550	0.46	608
	500	same	585	0.45	650
60	100	0.00008	450	0.75	470
	300	same	515	0.95	545
	500	same	560	0.87	595
90	100	0.00008	435	0.76	500
	300	same	520	0.87	540
	500	same	550	0.8	600

This method with the semi-empirical equation (Eq. C-1) provides a convenient way to determine the initial eccentricity for achieving a 25-year lifetime based on orbit and spacecraft conditions at end-of-life. The required ΔV or propellant for orbit insertion can then be computed (see Figure C-4 as an example). The value of eccentricity determined by this method may be verified using either Method 1 (previously-generated results) or Method 2 (semi-analytical integration) discussed in this report.
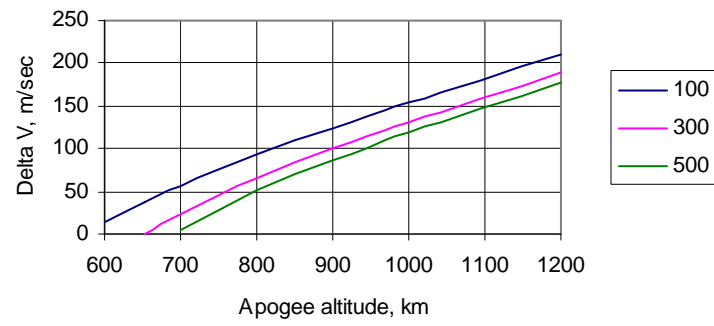
Figure C-4. ΔV vs. initial apogee altitude for achieving 25-year lifetime at 30 deg inclination with $C_DA/m = 100$, 300 and 500 cm^2/kg.

Appendix D: Orbit Lifetime Sensitivity to Sun-Synchronous, Magic, Molniya Orbits and Thermospheric Global Cooling

D.1 Orbit Lifetime

For sun-synchronous orbits, orbit lifetime has some sensitivity to the initial value of RAAN due to the density variations with the local sun angle. Results of 25-year propagations using both JB2006 and MSIS2000 show similar trends—that orbits with 6:00 a.m. local time have longer lifetime than orbits with 12:00 noon local time by about 500 days. This maximum difference (500 days) translates into a 5% error. It is recommended that the long-term (25 year) lifetime prediction of a sun-synchronous orbit should be performed only by a semi-analytical or numerical integration tool.

For Molniya orbits, iteration has been found to be difficult when computing the 25-year lifetime due to the coupling in eccentricity between the third-body perturbations and the drag decay. Figure D-1 shows the 15-year history of perigee altitude of a particular Molniya orbit with an initial RAAN of 97 deg. The long-term (7-year) sinusoidal variation is caused by the third-body attractions on orbit eccentricity. The perigee variation can be out of phase by 90 degrees if the initial RAAN becomes 7 deg. The atmospheric drag force becomes significant only when the perigee is considerably below 800 km. The strong sensitivity to initial RAAN and epoch makes it difficult to estimate the 25-year lifetime using empirical equations. Similar to the Sun-synchronous orbits, it is recommended that Method 2 or 3 be used when assessing the initial conditions that will achieve a 25-year lifetime for this type of orbit.
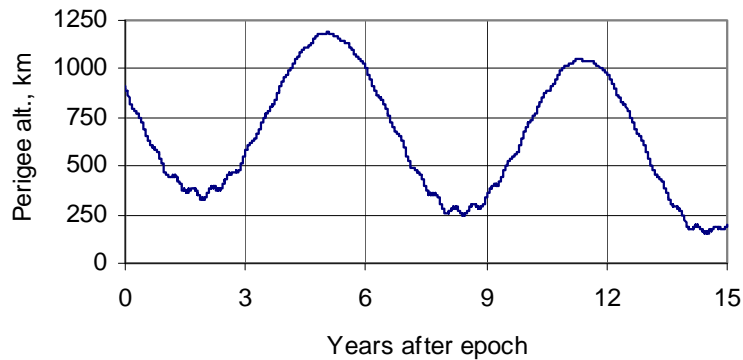

Figure D-1. Perigee altitude history of a Molniya orbit.

The so-called 'Magic' orbit is defined as having a three-hour period with a repeating ground track, where the orbit is highly-elliptical, critically-inclined and Sun-synchronous. A typical Magic orbit is given below:

a = 10572.87 km
e = 0.35
i = 116.565 deg
Ω = 45 deg
ω = 270 deg
M = 0 deg

Based on the above orbit, the maximum perigee altitudes (for not exceeding 25-year lifetime) for three selected ballistic coefficients (100, 300, 500 cm^2/kg) were determined using LIFETIME and plotted against local mean solar time of ascending node in Figure D-2. The strong sensitivity to initial RAAN is due to the sun-synchronous nature of the Magic orbit. The difference in initial perigee altitude of the disposal orbits can be as large as 180 km, depending on the difference in local mean solar time.
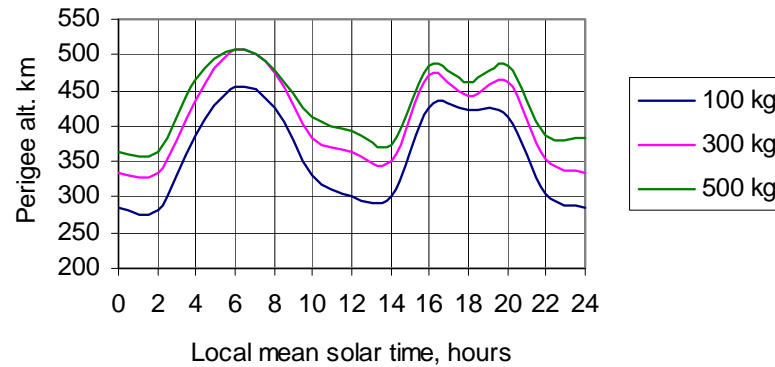

Figure D-2. Estimated perigee altitudes vs. local mean solar time of ascending node for Magic orbits.

Although the above figure (Figure D-2) can serve as a guide to determine the perigee altitude of a disposal orbit of a Magic orbit, it is again recommended that Method 2 or 3 be used when determining the 25-year lifetime for this type of orbit.

D.2 Implication of Observed Thermospheric Global Cooling

Recent indications of global cooling in the thermosphere may have a gradually increasing role in orbit lifetime estimation. The thermosphere is defined to occur roughly between 80 and 500 km altitude, which is a key part of the LEO regime for which the ISO standard is being developed. Both satellite measurements[28] and theoretical models[30, 31] indicate that the thermosphere is cooling off, causing density to lower. The mechanism causing this change appears to be that as CO_2 concentrations have increased (from 320 ppmv in 1965 to around 380 ppmv in 2005) at altitudes below 30km,[29] the upper atmosphere is correspondingly cooling down. It is estimated that because of this effect, atmospheric density will decrease by between 1.7%[26] and 2%[29, 30] per decade.

To study the implications of this finding, we placed a 1.7% per decade decrease into the LIFETIME and QPROP software programs. The results are shown in Figures D-3 and D-4. In Figure D-3, the orbit decay profiles for the equatorial (0 degree inclination) and polar (90 degree inclination) cases are compared for the current atmosphere model predictions (profiles 'A') and the atmosphere models with an overlaid thermospheric cooling density effect of 1.7% per decade. Figure D-4 contrasts with the sample case used in Figure B-2. In both cases, note that the introduction of the 1.7% per decade thermospheric cooling effect density decrease led to an orbit lifetime increase. Specific to the IADC-recommended 25-year orbit lifetime criterion, Figure D-3 shows a predicted lifetime increase of approximately 6–7%.
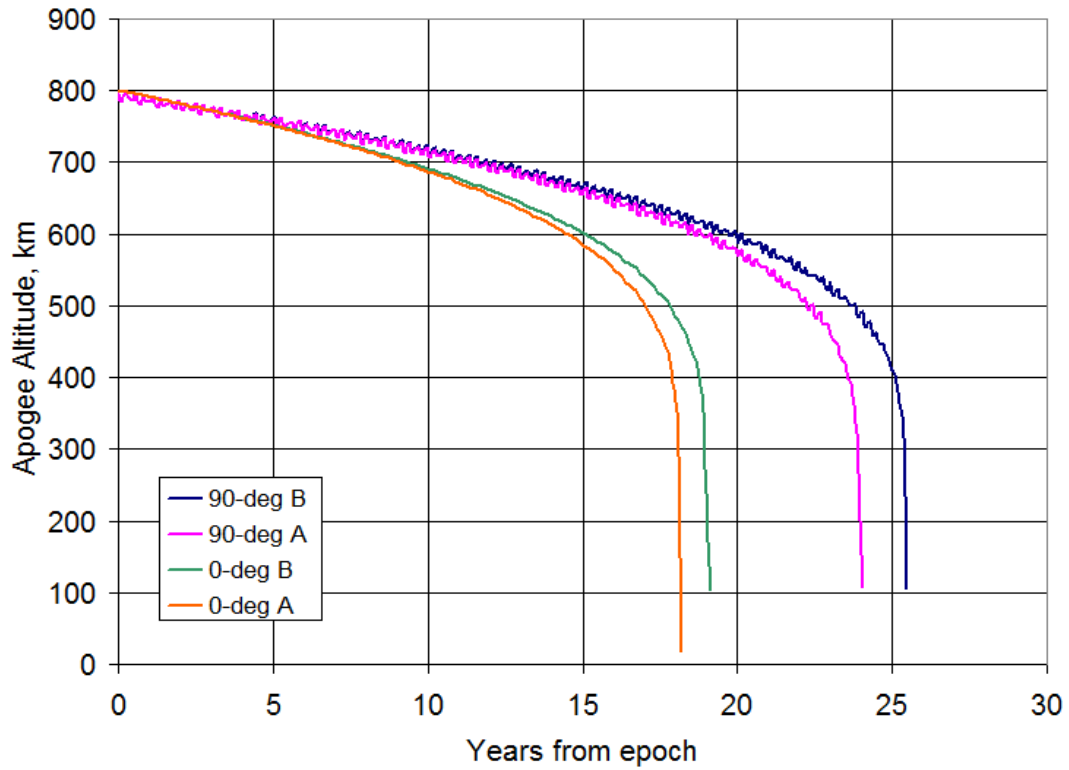
Figure D-3. Orbit lifetime estimates including and excluding thermospheric cooling
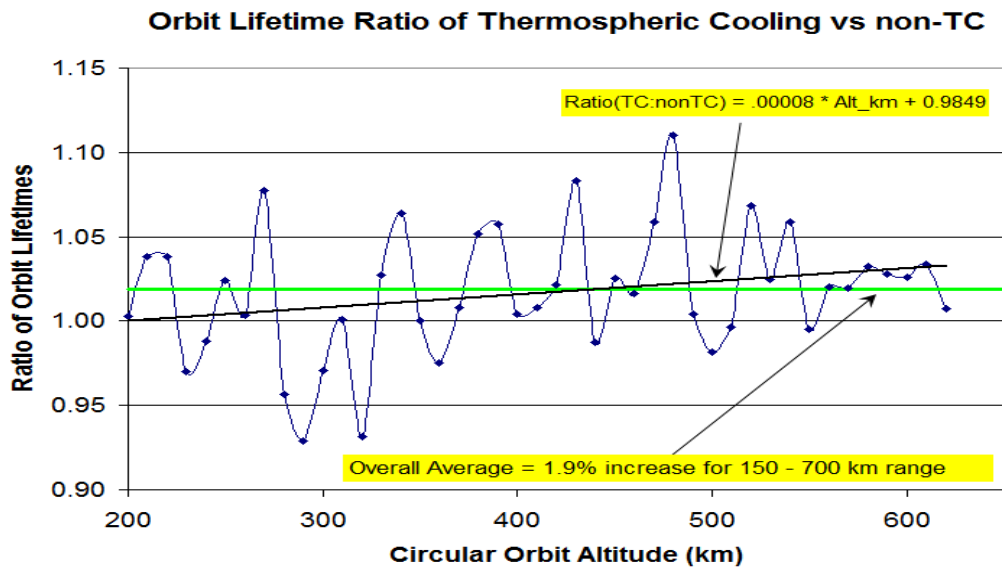for 0° & 90° inclination cases.

Figure D-4. Orbit lifetime variation induced by thermospheric global cooling effect
on sample case from Fig. B-2.

Appendix E: Discussion of Conditional Probability

The reliability requirement given in 6.2, "The space system shall be designed such that the probability of successful end-of-mission disposal, including depletion of energy sources, equals or exceeds 0,9 at the time disposal is executed," represents a typical and consistent approach to managing the multiphased mission from a probability point of view.

Assuming the orbital scenario is constituted by the following two main phases:

- Nominal mission (named *M*), and

- Disposal (named *D*).

the Conditional Probability Theorem allows us to state

$$P(M \cap D) = P(M) \times P(D/M) \qquad \text{(E-1)}$$

It follows that

$$P(D/M) = \frac{P(M \cap D)}{P(M)} \qquad \text{(E-2)}$$

Therefore, the probability, *P(D/M)*, of successfully performing the end-of-mission disposal once the nominal mission has been completed may be estimated starting from:

- *P(M)* = mission success probability (normally evaluated in the frame of the dependability program to verify the compliance of the developed design with regard to the applicable mission reliability requirement), and

- *P(M∩D)* = probability of correctly performing both mission and disposal phases. (This is generally an extension of the *P(M)* model.)

The following cases are presented to clarify the application of Equation (E-2).

E.1 Case 1

The end-of-mission disposal is performed making use of "all" subsystems involved in the nominal mission, as illustrated in the Venn diagram shown in Figure E-1.
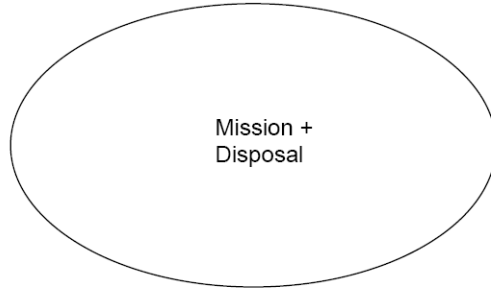
Figure E-1. All subsystems involved in the nominal mission required for disposal.

In this way, the reliability model defined for the nominal mission $[0; T_{mission}]$ is extended to cover both phases $[0; T_{mission} + T_{disposal}]$.

$$P(D/M) = \frac{R_{system}(T_{mission} + T_{disposal})}{R_{system}(T_{mission})} \tag{E-3}$$

E.2 Case 2

The end-of-mission disposal is performed making use of "some" subsystems involved in the nominal mission, as illustrated in the Venn diagram shown in Figure E-2.
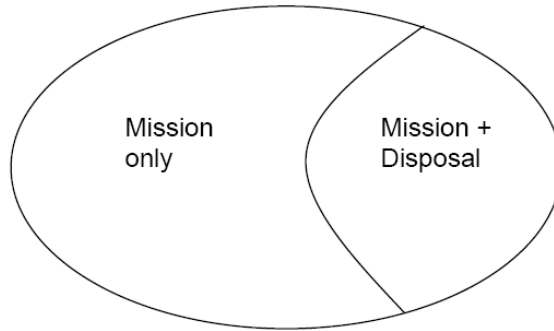

Figure E-2. Some subsystems involved in the nominal mission are used for disposal.

In this case, the function $R'_{system}(t)$ includes the reliability of the subsystems used for disposal estimated over the interval $[0; T_{mission} + T_{disposal}]$. For the remaining subsystems, the interval $[0; T_{mission}]$ is considered. For all subsystems, the reliability models defined for mission success may be used, even if with different time durations.

The reliability function $R_{system}(t)$ refers to the nominal mission (as presented in Case 1).

$$P(D/M) = \frac{R'_{system}(T_{mission} + T_{disposal})}{R_{system}(T_{mission})} \tag{E-4}$$

E.3 Case 3

The end-of-mission disposal is performed making use of dedicated equipment and "some" subsystems involved in the nominal mission, as illustrated in the Venn diagram shown in Figure E-3.
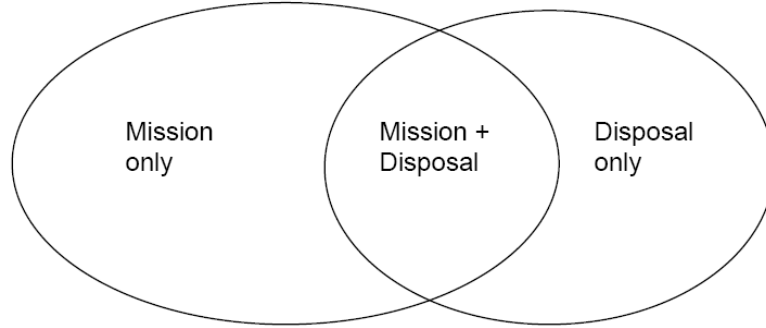

Figure E-3. Disposal requires some systems used for normal operations plus some systems specifically used for disposal only.

In this extension of Case 2, the $R''_{system}(t)$ function includes the contribution of the equipment for disposal: considered in active or passive mode (as applicable) in the interval $[0; T_{mission}]$ and in active mode in the interval $[T_{mission}; T_{mission} + T_{disposal}]$.

The reliability function, $R_{system}(t)$, refers to the nominal mission (as presented in Case 1).

$$P(D/M) = \frac{R''_{system}(T_{mission} + T_{disposal})}{R_{system}(T_{mission})} \qquad \text{(E-5)}$$

Several cases may be described. The cases presented in this appendix are provided to clarify the approach taken in this standard.

SMC Standard Improvement Proposal

INSTRUCTIONS

1. Complete blocks 1 through 7. All blocks must be completed.
2. Send to the Preparing Activity specified in block 8.

NOTE: Do not use this form to request copies of documents, or to request waivers, or clarification of requirements on current contracts. Comments submitted on this form do not constitute or imply authorization to waive any portion of the referenced document(s) or to amend contractual requirements. Comments submitted on this form do not constitute a commitment by the Preparing Activity to implement the suggestion; the Preparing Authority will coordinate a review of the comment and provide disposition to the comment submitter specified in Block 6.

SMC STANDARD CHANGE RECOMMENDATION:	1. Document Number	2. Document Date
3. Document Title		

4. Nature of Change
(Identify paragraph number; include proposed revision language and supporting data. Attach extra sheets as needed.)

5. Reason for Recommendation

6. Submitter Information

a. Name	b. Organization
c. Address	d. Telephone
e. E-mail address	7. Date Submitted

8. Preparing Activity	Space and Missile Systems Center
	AIR FORCE SPACE COMMAND
	483 N. Aviation Blvd.
	El Segundo, CA 91245
	Attention: SMC/EAE

March 2008